ELSEVIER

Tectonophysics 286 (1998) 273–298

TECTONOPHYSICS

Waves of the future: Superior inferences from collocated seismic and electromagnetic experiments

Alan G. Jones *

Geological Survey of Canada, 1 Observatory Crescent, Ottawa, Ont. K1A 0Y3, Canada

Received 11 February 1997; accepted 10 July 1997

Abstract

The advent of high-quality seismological studies of the Earth's continental lithosphere has been paralleled by an explosion in both the quality and quantity of concomitant high-resolution electromagnetic studies. The latter were inspired by technological and intellectual advances during the last decade in the acquisition, processing, modelling and inversion of particularly natural-source magnetotelluric (MT) data. The complementary nature of seismics and MT leads to rejection of hypotheses that may be tenable if only one of them is applied. Equally, inferences supported by both have stronger conviction. Perhaps most useful is when apparent incompatibilities must be reconciled by re-examination of both datasets. This is demonstrated through examples of magnetotelluric and seismic reflection studies undertaken in the last decade in many tectonic environs, from Palaeoproterozoic collision zones to passive margins to active collision zones. Some aspects of MT are explained, particularly the method's sensitivity and resolution of geoelectric directionality and dimensionality. New directions are proposed whereby greater utility of the joint datasets can occur, both at the outset during data acquisition, and in the interpretation phase in modelling and inversion. Also, laboratory measurements of seismic, electrical and rheological properties of the same rock sample will make integrated interpretation more tenable.

Keywords: seismic surveys; electromagnetic surveys; physical properties; continental crust

1. Introduction

Imaging structures within, and determining the state and properties of, the continental lithosphere continue to be important milestones in our attempt to understand the processes that created and modified the lithosphere. Many of the world's geoscientific efforts in this endeavour are spearheaded by the innovative use in crystalline terranes of seismic reflection technologies adapted from petroleum exploration. Coupled with seismic acquisition, some national and international programs also include non-seismic methods, for example the Canadian Lithoprobe programme (Clowes et al., 1993), the U.S. National Science Foundation's Continental Dynamics programme (CD/2020, Phinney et al., 1993), the European Europrobe programme, and the German Continental Deep Drilling programme (Kontinentales Tiefbohrprogramm, KTB) (Emmerman and Lauterjung, 1997). Unequivocally, these ancillary multidisciplinary studies add value to the interpretation of the seismic data by providing supporting evidence or, on occasion, suggesting alternative, viable interpretations.

* Corresponding author. Fax: +1 613 992 8836. E-mail: jones@cg.nrcan.gc.ca

0040-1951/98/$19.00
PII S0040-1951(97)00270-9

Table 1
Collocated seismic and MT experiments conducted during the last decade

Continent/Region	Location	Geological problem	Project	References[a]
Africa	Kenya	Active rift	KRISP	Simpson et al. (1996)
Antarctic	Byrd Basin	Active rift (?)		Clarke et al. (1998); Wannamaker et al. (1996)
Asia	Tibet	Continent–continent collision (India–Asia)	Indepth	Nelson et al. (1996); Chen et al. (1996)
Asia	Pakistan	Uplifting core complex (Nanga Parbat)		Meltzer et al. (1996); Park and Mackie (1996)
Atlantic Ocean	North Atlantic	Spreading ridge (Reykjanes Ridge)	RAMASSES	Sinha et al. (1997); Constable et al. (1997)
Europe	Finland	Palaeoproterozoic granulite belt (Lapland Granulite Belt)	EGT	Korja et al. (1996)
Europe	Sweden and Norway	Mountain belt evolution (Caledonides)		Hurich et al. (1989); Gharibi and Korja (1996); Gharibi et al. (1997)
Europe	Finland, Norway and Sweden	Archaean Shield (Fennoscandia)	EGT BABEL	Korja et al. (1993)
Europe	Germany	Rhenish Massif	DEKORP	Franke et al. (1990); Volbers et al. (1990)
Europe	Germany	Site characterization	KTB	Haak et al. (1997); Harjes et al. (1997)
Europe	Hungary	Bohemian Massif		Aric et al. (1998)
Europe	Hungary	Deep structure of extensional basins (Pannonian Basin)	PANCARDI (PGT)	Posgay et al. (1996); Adam et al. (1996); Adam (1997)
Europe	Spain	Betic	ESCI	Pous et al. (1996)
Europe	France	Cadomian orogeny	GeoFrance3D	Groupe ARMOR (1998)
Europe	Ireland	Variscides	VARNET	
New Zealand	South Island	Southern Alps	SIGHT	Ingham (1996); Jiracek et al. (1996b); Holbrook et al. (1996); Davey et al. (1998); Stern et al. (1998)
North America	California	Sierras	SSCD	Fliedner et al. (1996); Park and Mackie (1996); Wernicke et al. (1996)
North America	Saskatchewan, Manitoba and North Dakota	Palaeoproterozoic orogen (Trans-Hudson)	Lithoprobe	Lucas et al. (1993); Jones et al. (1993b)
			Cocorp	Nelson et al. (1993); Booker et al. (1997)
North America	Southern British Columbia	Canadian Cordillera	Lithoprobe	Cook (1995); Jones and Gough (1995)
North America	California	Active strike-slip fault (San Andreas)	SAF studies	Mackie et al. (1996); Unsworth et al. (1997)
North America	Alberta	Basement structures	Lithoprobe	Ross et al. (1995); Boerner et al. (1995)
North America	Ontario	Uplifted middle crustal block (Kapuskasing Uplift)	Lithoprobe	Leclair et al. (1994); Mareschal et al. (1994); Percival and West (1994)
North America	Quebec and Ontario	Mantle anisotropy	Lithoprobe	Mareschal et al. (1995); Senechal et al. (1996); Ji et al. (1996)
North America	West Coast	Oceanic subduction (Juan de Fuca plate)	EMSLAB USGS DCS	Wannamaker et al. (1989a,b); Trehu et al. (1994)
North America	New Mexico	Continental volcano	JTEX	Lutter et al. (1995); Jiracek et al. (1996a)

Table 1 (continued)

Continent/Region	Location	Geological problem	Project	References[a]
North America	Southwestern U.S.	Metamorphic core complex	PACE	Klein (1991); McCarthy et al. (1991)
North America	Nevada	Ruby Mountains	NSF CD	Stoerzel and Smithson (1996)
North America	Mexico	Chicxulub impact crater		Arzate et al. (1996)
North America	Mexico	Oceanic plate subduction (Cocos)	GEOLIMEX	Arzate et al. (1995)
South Pacific	Garrett segment	Melt migration and origin beneath mid-ocean ridge (East Pacific Rise)	MELT	Forsyth and Chave (1994)

[a] References given to the major review or overview paper where written.

This paper will describe the symbiotic relationship that can exist between crustal-scale seismic experiments and collocated electromagnetic (EM) studies. Whereas ten years ago there were few joint surveys (Jones, 1987), since then collocated seismic and magnetotelluric (MT) experiments have been conducted on almost all continents (Table 1). The considerable power of the Earth's natural time-varying electromagnetic field, and its almost ubiquitous extent, make MT the obvious choice for inexpensive, and logistically simple, deep EM investigations. A search with the joint keywords *seismic reflection* and *magnetotelluric* reveals over 300 papers and abstracts published since 1986, and the larger projects are listed in Table 1. It is not the purpose of this paper to review that vast body of literature, but rather to pick examples illustrating where superior inferences have resulted from combined interpretations. It should be noted that such joint interpretations are only of value when the seismic and electrical properties are correlated in some fashion. Seismic interpretations from images of a high seismic impedance contrast between rocks of equal electrical conductivity are not aided or further constrained by the inclusion of EM data, and an example of such a case is discussed below.

The sensitivity of electrical conductivity to the presence of small amounts of interconnected fluid makes EM methods particularly suitable for studies in geologically 'young' areas, such as Tibet and North America's Cordillera. Such studies may also address the rheological properties of the crust (see, e.g., Jiracek, 1985; Gough, 1986). However, in older areas, EM methods image metasediments containing interconnected conducting phases, such as graphite, sulphides and iron oxides (e.g., Duba et al., 1994). These metasediments can play an important role in defining the present geometry of structures and can contribute towards unravelling the tectonic history of the region.

Deducing the probable cause of the observed enhanced conductivity usually cannot be undertaken without reference to other information and accordingly hypotheses from EM images, just like those from seismic images, are strengthened when other information supports them, and weakened when they do not. Some studies have determined the most likely cause of enhanced current flow, such as that of Jones et al. (1997) which defines the North American Central Plains (NACP) conductivity anomaly as due to pyrite grains concentrated in the hinges of folds and connected along strike. However, interpretations from resistivity models alone are certainly not unique.

This paper is structured into three sections. First, some aspects of MT, perhaps not widely known by non-experts, are described. These aspects pertain to the method's ability to sense geoelectric dimensionality and directionality as potential proxies for structural dimensionality and directionality, both of which are important given the usual assumption made when interpreting seismic or EM data from a profile in a two-dimensional (2D) manner. Second, examples will be chosen from those in Table 1 to illustrate how seismics and EM together can give superior inferences on aspects of the crust and mantle. These examples are drawn from material that I am most familiar with, but are representative of what can be accomplished. Finally, a short section concludes on the proposed future of joint studies using new tech-

nologies becoming available, both instrumental and numerical.

The reader should note that the seismological studies are taken not just from vertical incidence reflection profiling, but from the whole spectrum of both active and passive source techniques, such as wide-angle reflection/refraction, conventional refraction, microearthquakes, and analyses using distant earthquake sources.

2. Magnetotelluric method

General information on the magnetotelluric method can be found in, for example, Vozoff (1986, 1991) and Jones (1992, 1993a). Those papers tend to dwell on the resolving power of the method, and on structural features of the models that can be derived, and the reader is directed to them for these points as they will not be repeated here. Aspects that have been somewhat less explained are the ability of MT data to sense the dimensionality of the subsurface, and to define directionality indicators. Obtaining these estimates at various frequencies indicates their variation laterally and with depth, and so indicates whether the typical 2D assumptions made are valid for the whole volume of investigation, part of it, or are not appropriate at all.

This sensitivity to dimensionality and directionality comes from the tensor nature of the observations obtained. Measurement is made at a location of the three time-varying components of the Earth's magnetic field (h_x, h_y, h_z) and the two horizontal components of the electric (telluric) field (e_x, e_y) measured on the Earth's surface. In the frequency domain, the 2×2 complex MT impedance tensor, $\mathbf{Z}$, relates the amplitude and phase of the horizontal components of the magnetic field ($H_x(f)$, $H_y(f)$) to those of the electric field ($E_x(f)$, $E_y(f)$), at a given frequency, f:

$$\begin{bmatrix} E_x \\ E_y \end{bmatrix} = \begin{bmatrix} Z_{xx} & Z_{xy} \\ Z_{yx} & Z_{yy} \end{bmatrix} \begin{bmatrix} H_x \\ H_y \end{bmatrix} \tag{1}$$

(dependence on frequency assumed for clarity) and this tensor can be analysed for directionality and dimensionality. From the complex impedance elements, one can define a scaled magnitude and the phase of the impedance element. For example, for the $Z_{xy}(f)$ element, the XY apparent resistivity and phase are given by:

$$\rho_{a,xy}(f) = |Z_{xy}(f)|^2 / 2\pi f \mu$$

$$\phi_{xy}(f) = \arctan[Im(Z_{xy}(f)]/Re[Z_{xy}(f)]$$

(μ is the magnetic permeability, usually taken as the free space value) and for a uniform half-space the XY and YX apparent resistivities become frequency independent and give the true electrical resistivity (inverse of conductivity) of the half space, and their impedance phases are 45° at all frequencies.

For a layered one-dimensional (1D) Earth, then $Z_{xx} = Z_{yy} = 0$, and $Z_{xy} = -Z_{yx}$ (the minus sign ensures a consistent right-hand coordinate system), and the apparent resistivities and phases as a function of frequency can be interpreted into variation of resistivity with depth. As a consequence of the *Skin Depth* phenomenon of EM fields, penetration into a medium is inversely proportional to the square root of the frequency of the incident wave. So information about the near surface is obtained from the high-frequency data, and about the deep structure from the low-frequency data. Phases > 45° indicate a transition to a less resistive zone with increasing depth, whereas phases <45° indicate a transition to a more resistive zone.

In the early days of the MT method, after it was proposed independently by Tikhonov (1950) and Cagniard (1953), only a scalar description existed whereby the Earth responses were derived from ratios of the perpendicular components of the EM field, e.g., $Z_{xy} = E_x/H_y$. This led to results that were not reliable and gave models that were not in agreement with those obtained from global spherical harmonic analyses of the geomagnetic field (Lahiri and Price, 1939; Migaux et al., 1960). A tensor relationship between the field components, as in Eq. 1, was first proposed by Neves (1957) and Berdichevsky (1960), and such a tensor describes fully the electrical conductivity variation of the subsurface, both vertically and laterally.

Over a 1D Earth, the MT tensor is rotationally invariant, and correctly indicates that the resistivity at a given depth, i.e., for a given frequency, is independent of the orientation angle. Resistivity varies with depth alone.

Respectively, over a 2D Earth, when the x and y axes are parallel and perpendicular to geoelectric

strike, $Z_{xx} = Z_{yy} = 0$, but $Z_{xy} \neq -Z_{yx}$. In an arbitrary coordinate acquisition system, not aligned with electrical strike, the diagonal terms are not zero. Accordingly, with noise-free data over a 2D Earth one can simply rotate the measured impedance tensor until it becomes purely anti-diagonal. This tensor is rotationally variant, and indicates that the lateral resistivity at a given depth is dependent upon the orientation angle. In the presence of noise, analytical and numerical methods were proposed to estimate, in some optimum manner, the appropriate strike direction, e.g., by numerically maximizing the magnitude-squared of one of the anti-diagonal elements (Bostick and Smith, 1962; Everett and Hyndman, 1967) or analytically maximizing the sum of the magnitude-squared of the two anti-diagonal elements (Swift, 1967). Geoelectric strike directions determined using these methods were not very satisfying, as they often varied wildly from frequency to frequency and from site to site, and were not consistent with surficial geological strike. Note that these older methods use the magnitude information in the impedance tensor elements, not the phase relation between the electric and magnetic field components.

The full three-dimensional (3D) problem occurs when all elements of the impedance tensor contain information. MT modelling and inversion is in its infancy for fully 3D data, and recently significant advances have been made using rapid, second-order approximations (e.g., Smith and Booker, 1991; Habashy et al., 1993), but 3D interpretations are not routine. However, a pivotal advance was realized with the appreciation that much of the MT data recorded, especially in crystalline terranes, exhibit the effects of distortions caused by galvanic charges on the boundaries of local, near-surface inhomogeneities. These distortions affect primarily the electric field and become frequency-independent, so cannot be avoided by recording at lower and lower frequencies. Thus, a physical model was developed of a distorting 3D thin sheet overlying a 2D regional Earth (3D/2D), and can be described mathematically as:

$$\boldsymbol{Z}_{\mathrm{obs}} = \boldsymbol{R}\,\boldsymbol{C}\,\boldsymbol{Z}_{\mathrm{2D}}\,\boldsymbol{R}^{T} \qquad (2)$$

where $\boldsymbol{Z}_{\mathrm{obs}}$ is the observed 2×2 complex impedance tensor, $\boldsymbol{R}$ is a 2×2 rotation matrix that rotates the true regional 2D response, $\boldsymbol{Z}_{\mathrm{2D}}$, into the observation reference frame, $\boldsymbol{C}$ is a 2×2 matrix of real, frequency-independent factors that describe the distortions on the electric field, and T represents transpose. This distortion model, first presented in conceptual form by Bahr (1984), has received widespread acceptance within the MT community after physical and statistical procedures for its estimation were proposed by Groom and Bailey (1989, 1991), and a methodology of its application was described by Groom et al. (1993). In contrast to earlier methods, this model relies upon the phase information within the impedance tensor, not the magnitude information, for deriving the strike direction.

Using the Groom–Bailey approach, one can analyze a given magnetotelluric impedance tensor for its directionality and dimensionality properties. If the impedance tensor is full, such that all elements contain independent information, then none of the above three models (1D, 2D, or 3D/2D) will fit the data to within the error tolerances. In this case the subsurface at the frequency band of interest is 3D. However, commonly the data are well described by the 3D/2D model, at least for part of the frequency range of observation, and one obtains the strike direction at that frequency (depth), and statistical confidence that the subsurface can be described by a 2D model at that frequency. An extension of this approach that uses multiple sites and multiple frequencies to determine the most consistent strike direction for most of the data was presented recently by McNeice and Jones (1996).

An example of the utility of the approach is given in Marquis et al. (1995). Directionality analyses of the MT data from south-central British Columbia, Canada, showed that the geoelectric strike has a significant depth-dependency (Fig. 1). The uppermost crust (to 7 km), derived from MT data in the frequency band 100–10 Hz (Fig. 1a), has an average strike direction of N25°W, consistent with surficial geological strike of the major morphogeological belts within the Canadian Cordillera. In contrast, most of the crust (7–34 km), exemplified by the MT data in the frequency band 1–0.1 Hz (Fig. 1b), displays an average strike direction that is very different, generally N20°E, and the uppermost mantle, determined from the frequency band 0.01–0.001 Hz (Fig. 1c), shows a different angle again, N60°E. The former is consistent with the strike of North American rocks where exposed in the Purcell Anti-

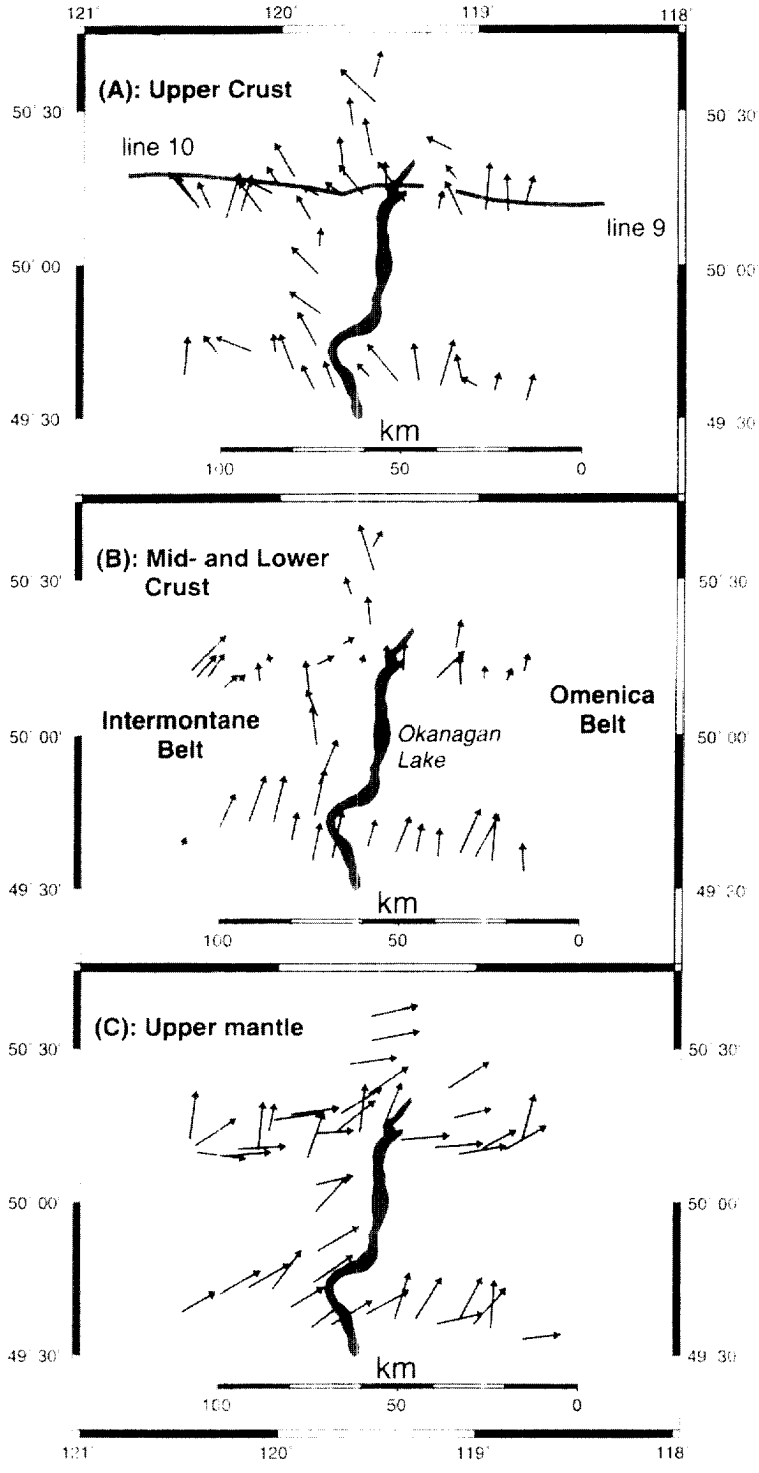
121°
120°
119°
118°
(A): Upper Crust
line 10
line 9
50° 30'
50° 00'
49° 30'
km
100
50
0
(B): Mid- and Lower Crust
Intermontane Belt
Okanagan Lake
Omenica Belt
(C): Upper mantle

clinorium, whereas the latter is consistent with the Juan de Fuca plate subduction direction.

Recent analyses of the seismic data from the region for reflectivity as a function of azimuth determined a large variability, with four persistent trends from the data in the range 0–12 s two-way travel time (TWTT), at (I) 025–040°, (II) 085–095°, (III) 115–125°, and (IV) 140–160° (320–340°) (Cook et al., 1997). Trends III and IV are interpreted to be associated with the regional middle Tertiary extensional fabric stretching direction of about 120°, and with the strike of regional contraction, respectively. Trend I was conjectured to be also possibly associated with the extension, with development of the flattening fabric causing reflectivity perpendicular to lineation. Trend II is not related to any known structural orientations in the region. The significance of trends IV and I being commensurate with the strike directions derived from the MT data for the upper and lower crust respectively, needs to be evaluated further. However, of note is the fact that MT data, by their *tensor* nature, are implicitly sensitive to dimensionality and directionality, whereas seismic data along a profile require both fortuitous crooked-lines and sophisticated processing to extract comparable information.

Thoughtful use of seismic and EM together is advocated, not adoption of a general rule '*whither goes seismics, there must go MT*' (or vice versa), and certainly joint interpretation must be approached with care. Clearly, only in the case of seismic impedance and electrical conductivity variation both occurring at an interface does joint interpretation make sense. For example, Occam's razor interpretation of anomalies seen in both can lead to pitfalls, as demonstrated by Cook and Jones (1995). Data acquired on the Earth's surface in southeastern British Columbia displayed high reflectivity and high conductivity in the upper crust, and the alluring temptation is to assume that these result from the same structure(s) or process(es). However, a borehole demonstrated that the high reflectivity resulted primarily from the interfaces between metasedimentary units and gabbroic sills, whereas the conductivity came from layered sulphides within the interlayered metasedimentary units. Detailed examination proved that the suspected spatial correlation of the two was unfounded.

An additional problem is that depth penetration by EM fields is not always assured if the crustal section contains significant quantities of conducting material. An example is the Purcell Anticlinorium in southeastern B.C. and northern Montana, where abundant highly conducting sulphides (resistivity of 1 S m or less) precluded penetration below a few kilometres, even for periods as high as 1000 s (Gupta and Jones, 1995). A second example is from southern Tibet, where the conducting and thick crust prevented sensitivity to mantle structure even for EM waves of 30,000 s period (Chen et al., 1996).

3. Examples

3.1. Examples 1: imaging fluids

Electrical conductivity is very sensitive to the presence of an interconnected fluid phase, either partial melt or aqueous fluid. A dry gabbro or granite at 500°C exhibits a resistivity in the laboratory of $>100{,}000\ \Omega$ m, whereas in the presence of saline fluid its resistivity drops five orders of magnitude to $<10\ \Omega$ m (Olhoeft, 1981; Shankland and Ander, 1983). In comparison, the effect of pressure on electrical properties is small, with partially molten rocks showing conductivities at pressures of 25 kbar approaching 70% of the zero pressure values (Tyburczy and Waff, 1983). Exploration for interconnected fluid phases using the appropriate electrical or electromagnetic method is therefore very efficient, as the effect on the response function is so significant (e.g., Gough, 1992).

Fig. 1. Strike directions for frequencies sampling different depth ranges in south-central British Columbia. (a) Strikes from the high-frequency band (100–10 Hz) which samples the upper crust (<8 km). (b) Strikes from a medium-frequency band (1–0.1 Hz) that samples the middle and lower crust (8–32 km). (c) Strikes from the low-frequency band (0.01–0.001 Hz) sampling the upper mantle (>32 km). The length of the arrow denotes how well a 3D/2D model is fit by the data, with the long arrows fitting acceptably, and the short arrows fitting poorly. The latter infers either that there are 3D regional structures present, or that the estimated data errors are too small resulting in poor model fit. The locations of seismic lines 9 and 10 are shown in (a), and the morphotectonic belts in (b). (Adapted from Marquis et al., 1995.)

Aqueous fluids have been proposed as the reason for the globally observed enhanced conductivity of the continental lower crust (see, e.g., Jones, 1992; Hyndman et al., 1993), although there are strong objections from some in the petrological community (Yardley and Valley, 1997). This paper will not discuss that topic, but point out that the conducting continental lower crust is a major geoscientific conundrum that should be addressed by a coordinated and cooperative effort between geologists, geochemists and geophysicists.

Joint seismic and EM studies for fluids have not been restricted to land. Two recent experiments, one in the North Atlantic (RAMESSES, Table 1) and one in the South Pacific (MELT, Table 1) have as their objective imaging melts associated with spreading ridges.

3.1.1. Example 1.1: Garibaldi belt

A seismic reflection profile along the side of one of the Garibaldi volcanoes (Mount Cayley) in the Coast belt of British Columbia, a northward extension of the Cascades in Washington, imaged an unusually high-amplitude 'bright spot' between 4.15 s and 4.55 s two-way travel time (TWTT), equivalent to 12.5 to 13 km in depth, and extending 8 km laterally. This reflective package was initially attributed to magma or metamorphic fluids in the crust (Varsek et al., 1993), but careful study of the frequency and amplitude characteristics of the bright spot suggested to Hammer and Clowes (1996) that it more likely results from a fossil sill complex associated with the volcanic development of Mount Cayley.

Analyzing MT data recorded over the Garibaldi belt, Jones and Dumas (1993) were able to image three conductive features inferred to be associated with different types of fluids. The shallowest anomaly ('1' in Fig. 2a), of 20–100 Ω m, is interpreted as due to a fluid-dominated montmorillonite clay cap layer above the resistive sericite geothermal zone. A pervasive conducting lower crust ('2' in Fig. 2b), of ~100 Ω m begins at about 14 km, and is interpreted to be due to metamorphic waters released by devolatization reactions as the Juan de Fuca plate to the west subducts beneath northwestern North America. These trapped fluids have been imaged beneath Vancouver Island both electrically (Kurtz et al., 1986, 1990) and seismically (Cassidy and Ellis, 1991, 1993), and electrically beneath Oregon as part of the EMSLAB experiment (Wannamaker et al., 1989a,b). The most dominant feature imaged is the laterally bounded high-conductivity zone within this region ('3' in Fig. 2b), of ~10–20 Ω m, beginning at a depth of ~14 km. This is thought to be the source magma chamber of the volcanic belt, and its depth to top correlates well with estimates of 8–15 km from geothermal studies (Blackwell et al., 1990). Its spatial location correlates precisely with the Mount Cayley bright spot.

Hammer and Clowes (1996) admit that the seismic data do not exclude the possibility of the reflective package resulting from melt lenses or saline fluids. A sill complex would not generate a region of enhanced conductivity, and so an integrated interpretation should favour a fluid explanation, with the magma chamber alternative being most plausible.

3.1.2. Example 1.2: Tibet

Another example of MT studies that have imaged fluids is the recent work undertaken in the southern part of the Tibetan Plateau as part of the INDEPTH program of study (Nelson et al., 1996). Seismic studies in the Lhasa block identified 'bright spots' in the reflection profiles along the Yangbaijan Graben at TWTT of 5 s to 6 s (Brown et al., 1997) which exhibited P–S conversions in the wide-angle data (Makovsky et al., 1997). MT studies in the region perpendicular to the graben imaged regions of high conductivity (<3 Ω m), not only in the graben ('2', beneath 'YG' in Fig. 3) but also outside the graben ('1' and '3' in Fig. 3), within a generally conductive middle crustal layer (14–200 Ω m) (Chen et al., 1996). These independent observations were interpreted as evidence for a partially molten middle crust beneath southern Tibet of regional extent (Nelson et al., 1996).

3.2. Examples 2: imaging faults

MT and seismics have been used successfully together to image the geometries of crustal structures. This is particularly true of faults, given that subvertical faults cannot be directly imaged seismically. Theoretical model studies demonstrate the advantages of acquiring and interpreting varied seismic and electrical data, particularly in the case of saline-

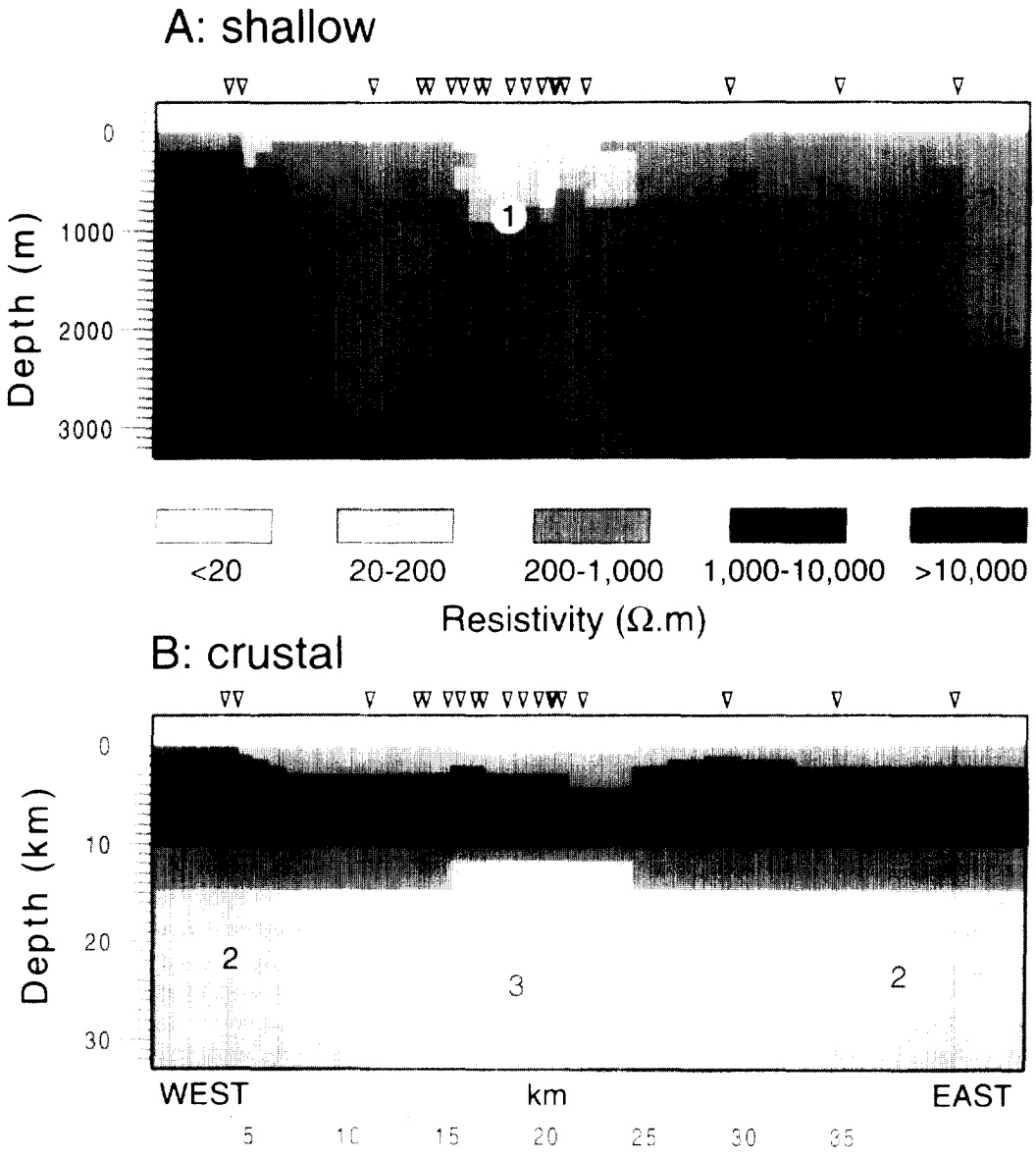

Fig. 2. Resistivity model obtained by 2D forward modelling MT data collected across the Garibaldi volcanic belt, the northward continuation of the Cascades, in southwestern British Columbia. The upper figure is of the shallow section (<3.3 km), whereas the lower figure is of the whole crust (to 33 km). Site locations shown by inverted triangles; *1* = shallow conducting region (20–100 Ω.m) associated with montmorillonite clay zone cap rock; *2* = pervasive low-resistivity (~100 Ω m) lower crust interpreted to be caused by metamorphic saline fluids; *3* = high-conductivity region (~10–20 Ω.m) thought to be the source magma chamber for the volcanic belt. (Adapted from Jones and Dumas, 1993.)

fluid-filled fault zones (Eberhart-Phillips et al., 1995). Faults can be imaged electromagnetically if they (a) contain saline fluids, (b) contain conducting metasediments, or (c) juxtapose rocks of differing resistivity. Below is given an example of each of these.

3.2.1. Example 2.1: San Andreas fault

The San Andreas fault is the best known continental strike-slip fault, and has been the subject of intense geophysical studies for over half a century. Subsequent to the 1989 rupture, the Loma

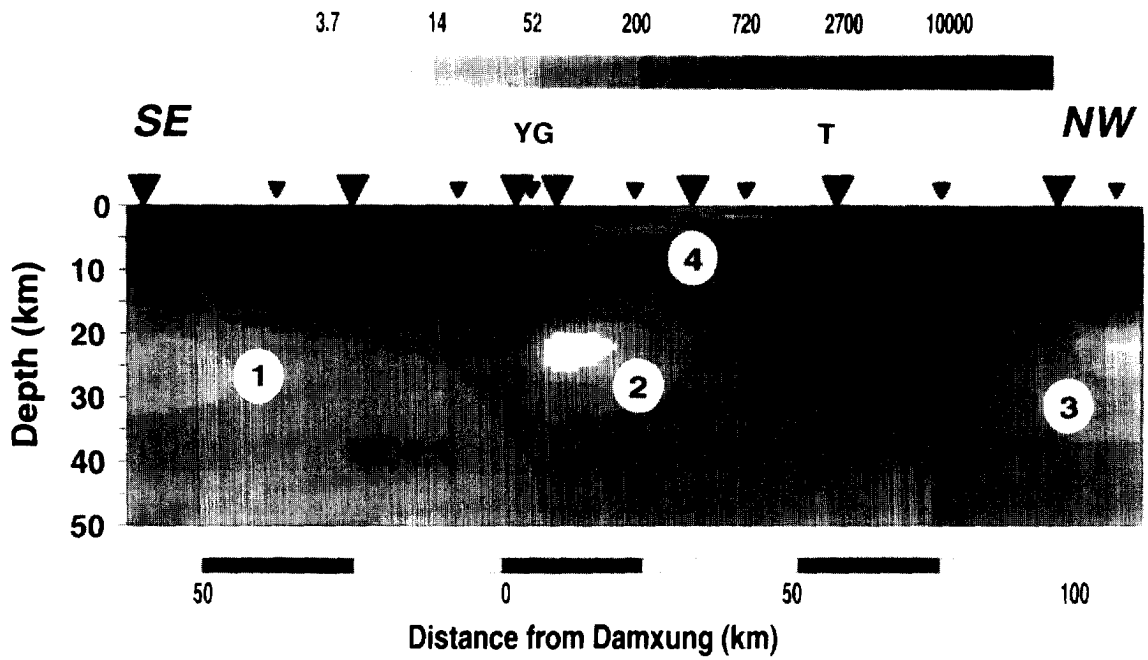

Fig. 3. Resistivity model from the MT profile crossing the Yadong–Gulu rift north of the Zangbo suture. Anomalies *1–4* imaged by MT. Anomaly *2* correlates spatially with a bright spot in the Yangbaijan Graben (*YG*). Anomalies *1* and *3* lie at the same depth but outside the graben. Anomaly *4* is a shallow anomaly from the town of Thak (*T*) dipping to the south ending on the southern flank of the graben. (Adapted from Chen et al., 1996.)

Prieta segment was studied using seismic and MT experiments, and a spatially collocated low velocity and low resistivity (<10 Ω m) zone, extending to depths >5 km, was imaged (Eberhart-Phillips et al., 1995). At Parkfield, a region of low resistivity and low velocity was also imaged (Eberhart-Phillips and Michael, 1993; Eberhart-Phillips et al., 1995), with the suggestion that the conductive fault zone extends through the whole crust (Park et al., 1991). These regional MT studies, with a wide MT station spacing, could not resolve a detailed fault zone structure.

Recently, a continuous profiling MT experiment, with sites 100 m apart rather than many kilometres as in the previous surveys, conducted across the fault at Parkfield, demonstrated the resolving power of MT for near-vertical structures (Unsworth et al., 1997). The resistivity model obtained (Fig. 4) shows the San Andreas fault zone to be an ~500 m wide, low-resistivity vertical zone down to 4 km, and is attributed to saline fluids present in the highly fractured fault zone. Observed microearthquakes and creep in the low-resistivity zone support the suggestion that seismicity at Parkfield is fluid driven.

3.2.2. Example 2.2: Fraser fault

The Fraser fault system (FF) in southwestern British Columbia is a Late Eocene strike-slip fault dextrally offsetting units by ~100 km (Coleman and Parrish, 1991). Together with its southerly extension in the state of Washington, the Straight Creek fault, it extends in a north–south direction for at least 500 km, and has been proposed as the southern segment of the 2000-km-long intracratonic Tintina–northern Rocky Mountain trench transform fault system (Price and Carmichael, 1986). The fault offsets the earlier Yalakom–Hozameen fault (YF and HF in Fig. 5). Between the YF and FF to the north lies the Stikine terrane, one of the largest of the exotic terranes that comprise North America's cordillera.

Data from a Lithoprobe seismic reflection profile (line 18, Fig. 5) were interpreted as suggesting three possible geometries for the Fraser fault (Varsek et al., 1993): a listric west-dipping geometry that soled into the mid-crust at about 6.3 s (trajectory FFA, Fig. 6); a broad zone of west-dipping reflectors that are located in the lower crust and possibly upper mantle (trajectory FFB, Fig. 6); and a high-angle crustal-

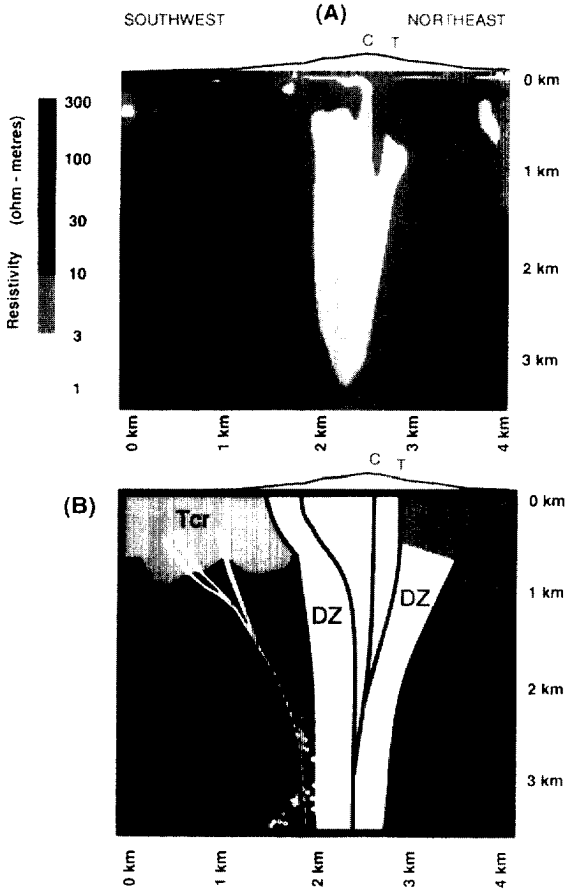

Fig. 4. Resistivity model of the San Andreas fault at Parkfield (top) and its cartoon interpretation (bottom): C = crest of Middle Mountain; T = creeping trace; Kg = Salinian granite; Kjf = Franciscan formation; Tcr = Coast Range sedimentary units; Tgv = Great Valley sedimentary units; DZ = fluid-saturated damaged zone. (Adapted from Unsworth et al., 1997.)

penetrating fault with west-side-down Moho offset (trajectory FFC, Fig. 6). Preference was expressed by Varsek et al. (1993) for geometry FFA, based on the apparent through-going reflective sequence at 6.3 s and from consideration of geological models for oblique deformation.

The MT data recorded over the FF suggest a different geometry (Jones et al., 1992). Phases at a period that sample the lower crust (10 s) show a distinct difference on either side of the fault to the south, the phases are higher (~72°) to the west and are lower (~60°) to the east (Fig. 5). To the north, the lower phases appear to follow the trend of the YF, rather than the FF. Thus, from the data alone, without sophisticated analyses or modelling, one can already draw significant conclusions about the likely geometry of the fault at depth. Inversion of the MT data from along the seismic reflection line gave a model with two orders of magnitude difference in resistivity in the lower crust on either side of the surface trace of the FF (Fig. 7), and imaged a zone of low resistivity in the fault zone within the mid-crust. The highly resistive Coast belt plutons west of the FF were also well imaged, with a depth extent of ~15 km. From the δD and δ^{13}C values recorded in the vicinity of the FF (Nesbitt and Muehlenbachs, 1991), the mid-crustal zone was interpreted as a region of enhanced organic carbon or graphite deposited during upwelling in the fault zone of deeply penetrating meteoric waters. Current concentration in this zone was mapped by the induction arrow responses at 3.5 s (Fig. 8), equivalent to depths of approximately a few kilometres, and are consistent with the surface trace of the FF and YF. Such current concentration has also been observed and mapped in another major strike-slip fault system, the crustal-penetrating Great Glen fault of Scotland (Kirkwood et al., 1981).

Interpretation of seismic refraction data recorded across the fault indicates a structural discontinuity in the wide-angle reflecting horizons of the lower crust beneath the surface location of the Fraser fault (McLean, 1995), consistent with the MT interpretation, although the lower crustal velocity does not appear to change from one side to the other (Clowes et al., 1995). Taking these MT results into consideration, the seismic reflection data were reprocessed using unconventional processing techniques to account for the severe crookedness of the line (see Fig. 5). One significant aspect of the reprocessed dataset was evidence of deep crustal extent, or possibly crustal penetration, for the Fraser fault (Perz, 1993).

The final integrated interpretation of the available seismological and MT data is of a near-vertical, deep-penetrating fault geometry (Fig. 6) (Cook, 1995).

3.2.3. *Example 2.3: Slocan Lake fault*

The Slocan Lake fault (SLF) in southeastern British Columbia is an Eocene extensional normal fault that accommodated crustal thinning and ex-

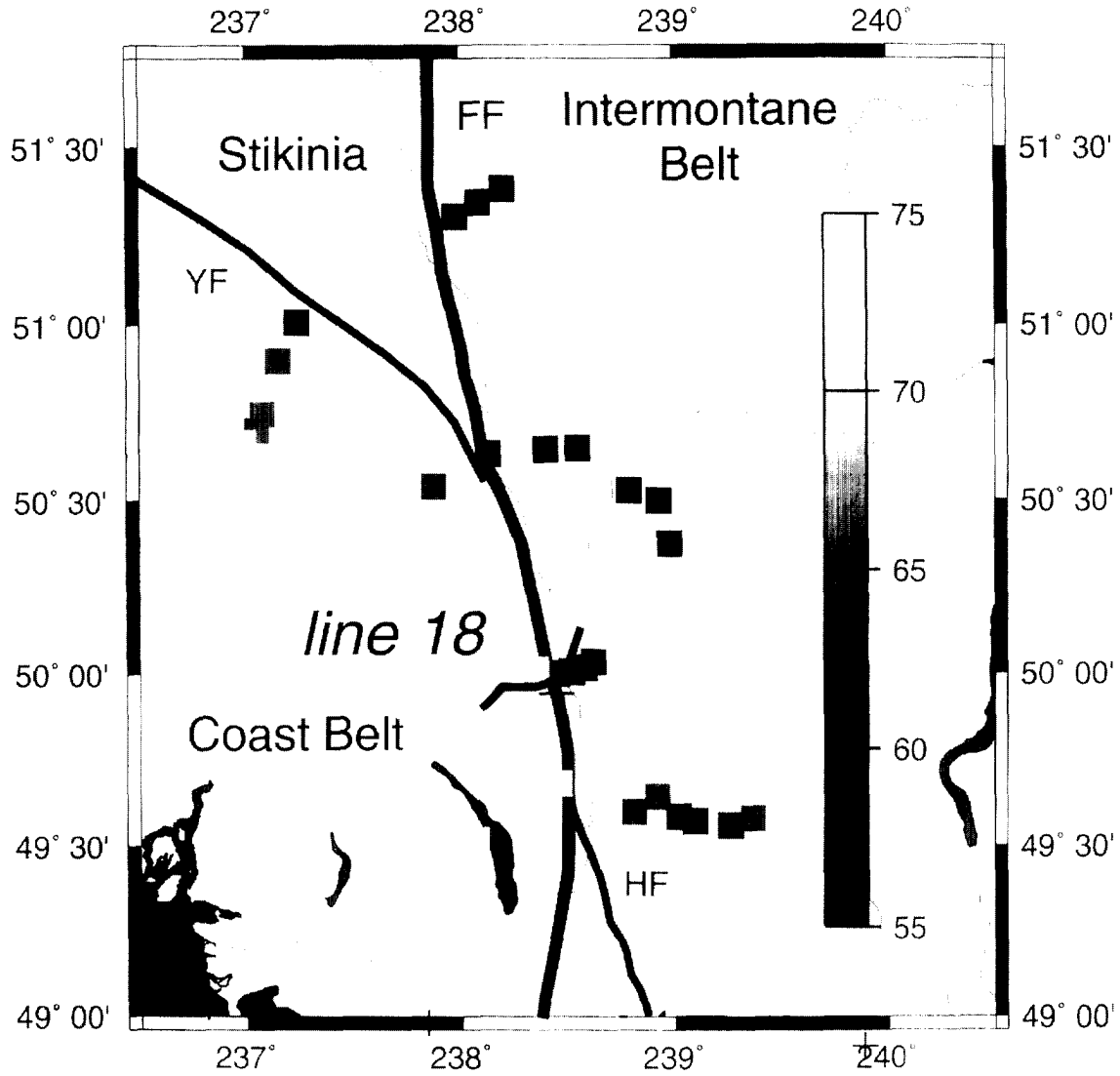

Fig. 5. Trace of the mid-Eocene Fraser fault (*FF*) and earlier Yalakom (*YF*) and Hozameen (*HF*) faults, together with the location of the MT sites (squares) and the seismic reflection profile (line 18). The squares are grey-shaded to indicate the effective phases at a period sampling the lower crust (10 s). Note that to the west of the FF and YF all phases are >70°, whereas to the east they are all <60°. (Adapted from Jones et al., 1992.)

posed the Valhalla gneiss metamorphic core complex in its footwall. At this location, it defines the boundary between two of British Columbia's morphogeological belts, the Omineca belt (OB) to the west and the Foreland belt (FB) to the east. The SLF is east-dipping, and is thought to be possibly crustal-penetrating and to cut and offset the Moho (Fig. 9). The reflection interpretation is that North American basement underlies the region in its entirety, and that the fault only offsets the basement (Cook et al., 1988, 1992).

This region has been investigated for over three decades using EM methods (see Jones, 1993b), as it was recognised by Hyndman (1963) in the early-1960s that a significant boundary in conductivity must exist to explain the differences in the observed

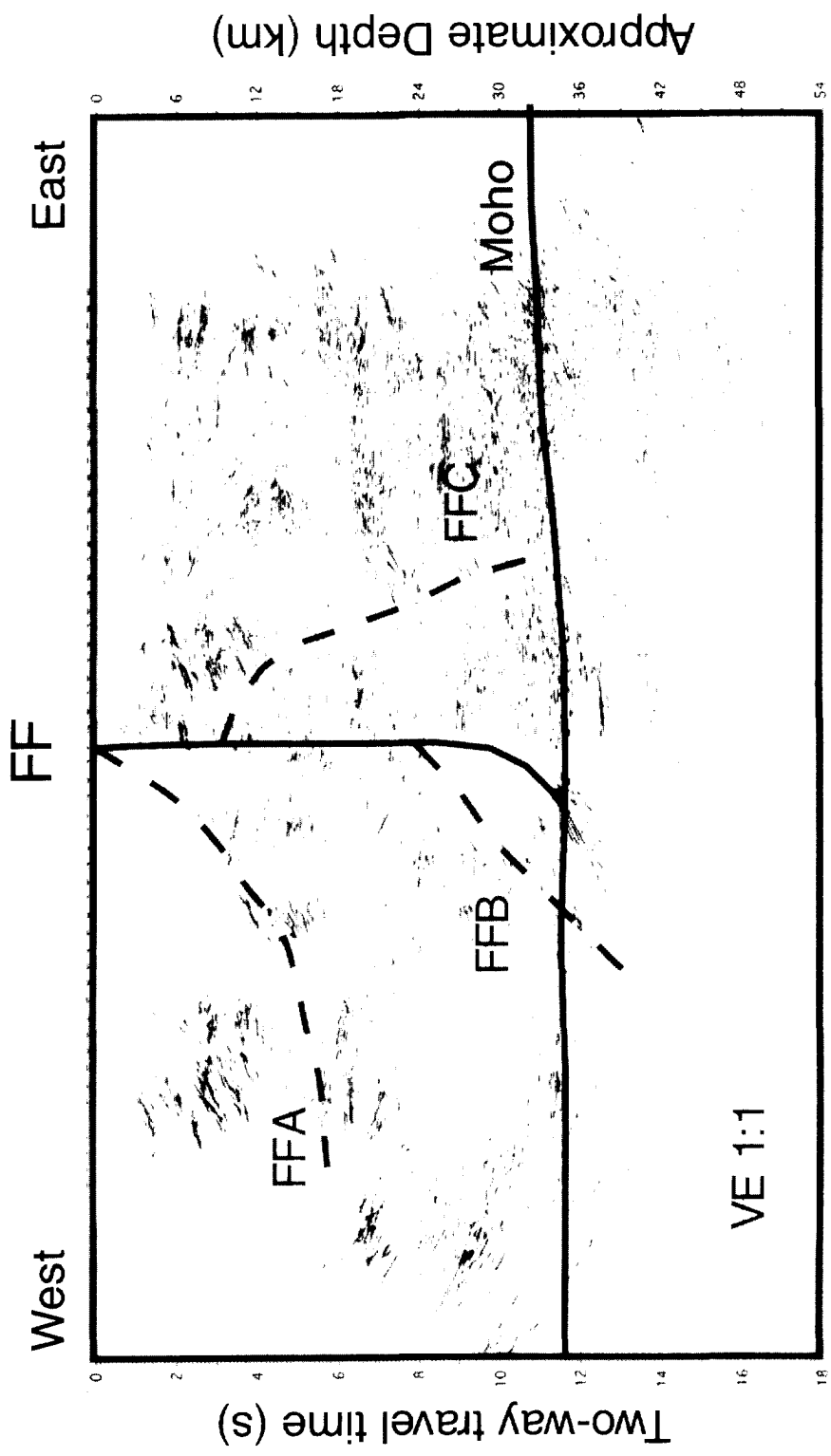

Fig. 6. Seismic reflection data from line 18 (Fig. 5) and three cartoon interpretations from Varsek et al. (1993) plus the Moho. The data are 1:1 for a velocity of 6 km/s. The vertical solid line traces the interpretation based on the MT results.

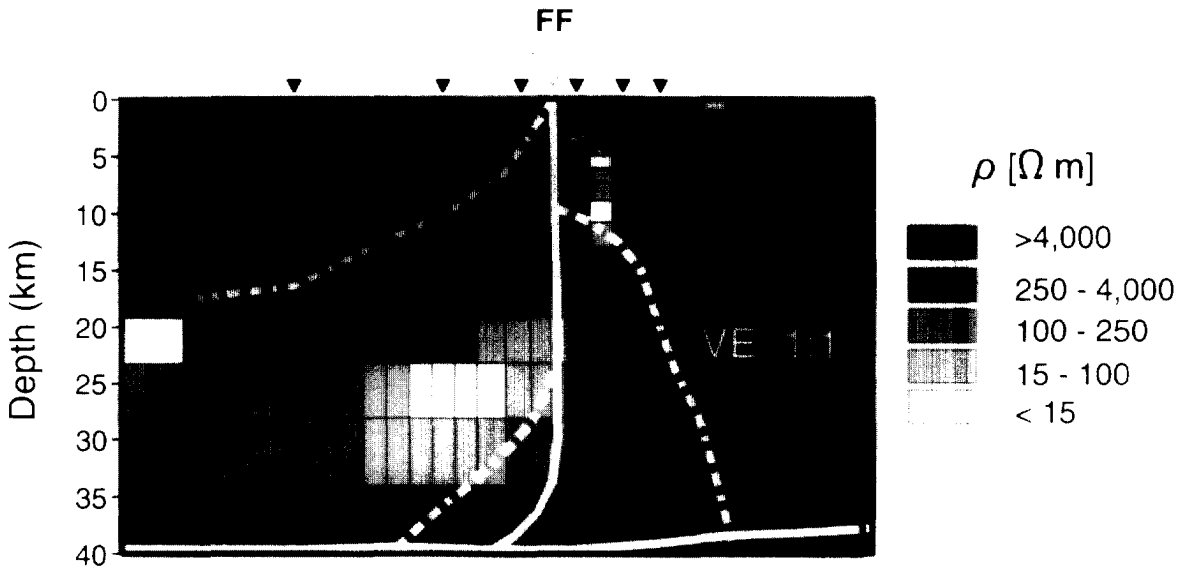

Fig. 7. Resistivity model obtained from the MT sites crossing the Fraser fault (*FF*) along line 18 (Fig. 5). The three trajectories from Fig. 6 are also imposed, as well as the suggested MT trajectory (white lines). Vertical exaggeration 1 : 1. (Adapted from Jones et al., 1992.)

ratios of the vertical to horizontal magnetic field amplitudes between sites in southern Alberta compared to southern British Columbia, Canada. Subsequent studies by Caner et al. (1967) confirmed Hyndman's observation. However, this 2D picture was shown to be too simplistic by a denser network of magnetometer sites around Kootenay Lake, southeastern British Columbia (Lajoie and Caner, 1970). The responses were modelled in terms of a three-dimensional lower crustal transition zone, with a resistive (250–1000 Ω m) lower crust to the east of Kootenay Lake, and a conductive (~5 Ω m) lower crust to the west and south. The Lithoprobe MT data from along the seismic lines display a strong change in impedance phase at periods sampling the lower crust (10–100 s), with high phases (60°–75°) to the west, and lower phases (30°–45°) to the east (Fig. 10), indicating a difference in the resistivity of the lower crust for the two regions (Jones et al., 1988). The resistivity model of the MT data has a change of half an order of magnitude in the resistivity of the lower crust at approximately the location of the SLF (Fig. 11) (Jones et al., 1993a).

This change in resistivity is accompanied by a change in seismic velocity. Zelt and White (1995) model the Lithoprobe seismic refraction data from the region, and show a change on either side of the SLF with faster P-wave velocities to the west beneath the OB (6.6–6.7 km/s) compared to the east beneath the FB (6.2–6.5 km/s) (Fig. 9). The surprisingly low velocities beneath the FB are difficult to explain, and a more felsic lower crust was suggested by Zelt and White (1995). The correspondingly more mafic lower crust beneath the OB does not explain the observed resistivity decrease.

Clearly, if 'North American' basement continues to the west of the SLF, it is modified by reworking, possibly as a consequence of underplating. An alternative explanation is that the basement west of the SLF is not North American, but was attached to the exotic terranes that docked with North America.

3.3. Example 3: imaging orogens

The Palaeoproterozoic Trans-Hudson orogen (THO) in the U.S. Dakotas, and Saskatchewan and Manitoba in Canada welded together the Superior, Wyoming and Rae/Hearne cratons (Fig. 12). EM studies played a large part in the discovery of its continental scale and, in fact, Camfield and Gough (1977) were the first to propose that a suture zone lay beneath the thick sediments in the mid-continent

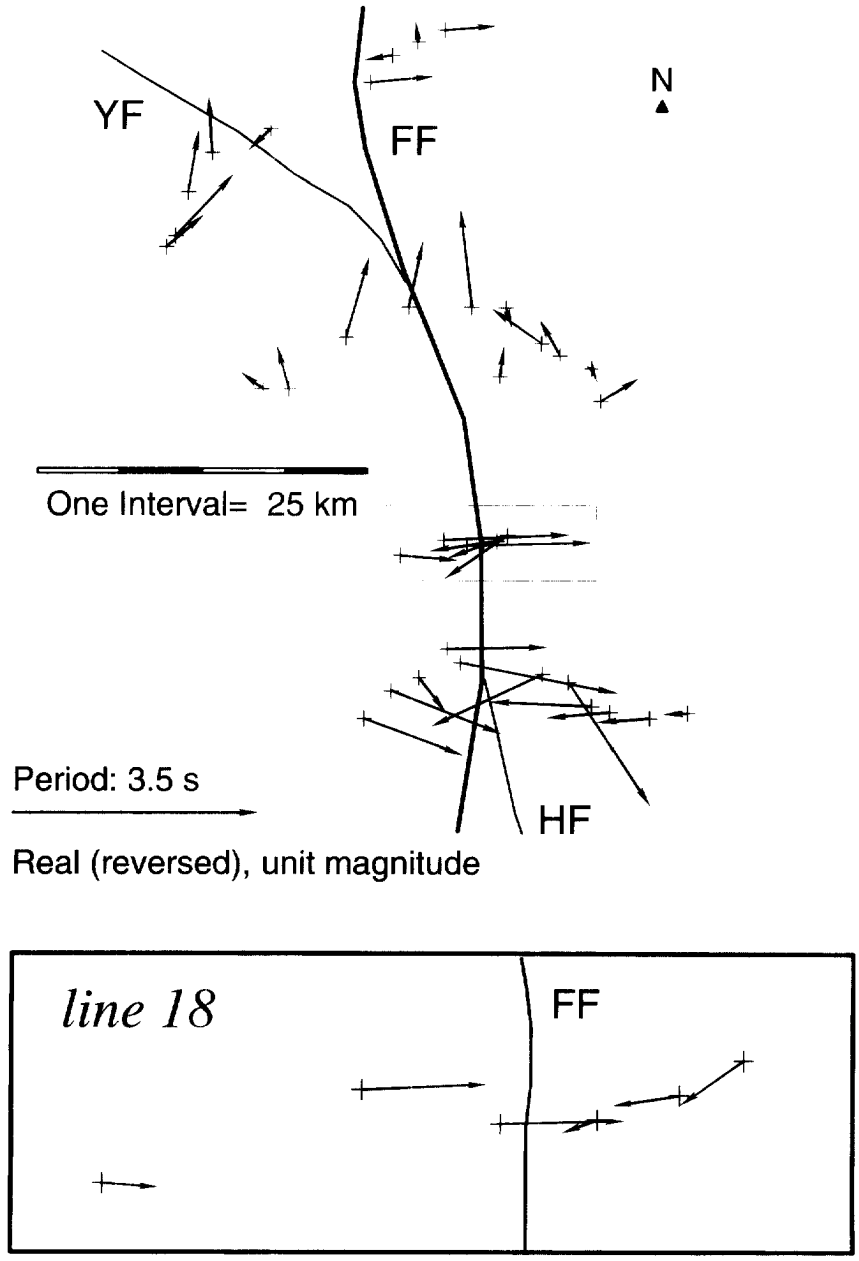

Fig. 8. Real induction arrows (reversed) at 3.5 s period. Note the reversal in the arrows where the faults are, indicating the presence of currents concentrated in the fault zones. (Adapted from Jones et al., 1992.)

of North America. This was based on magnetometer array studies through the 1960s and 1970s that identified an elongated and narrow zone of electric current concentration running from the Black Hills of southern South Dakota to northern Saskatchewan, named the North American Central Plains (NACP) conductivity anomaly (see references in Camfield and Gough, 1977). This current must flow in an anomalous body of enhanced conductivity. Subsequent profiles in northern Canada demonstrated that

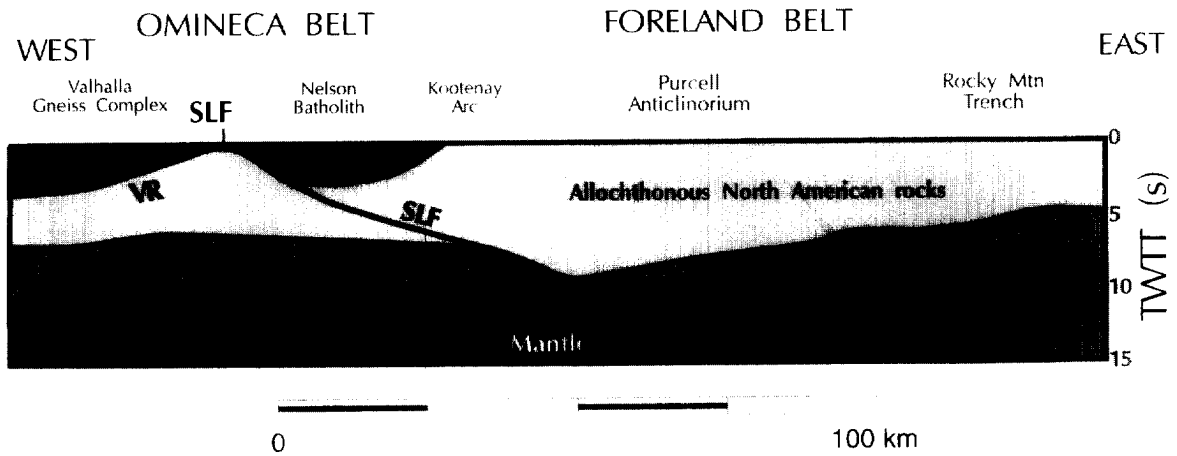

Fig. 9. Geometry of structures in southeastern British Columbia based on the seismic reflection results of Cook et al. (1988). Velocities for the lower crust determined by Zelt and White (1995). *SLF* = Slocan Lake fault. *VR* = Valhalla reflector. (Adapted from Jones, 1993b.)

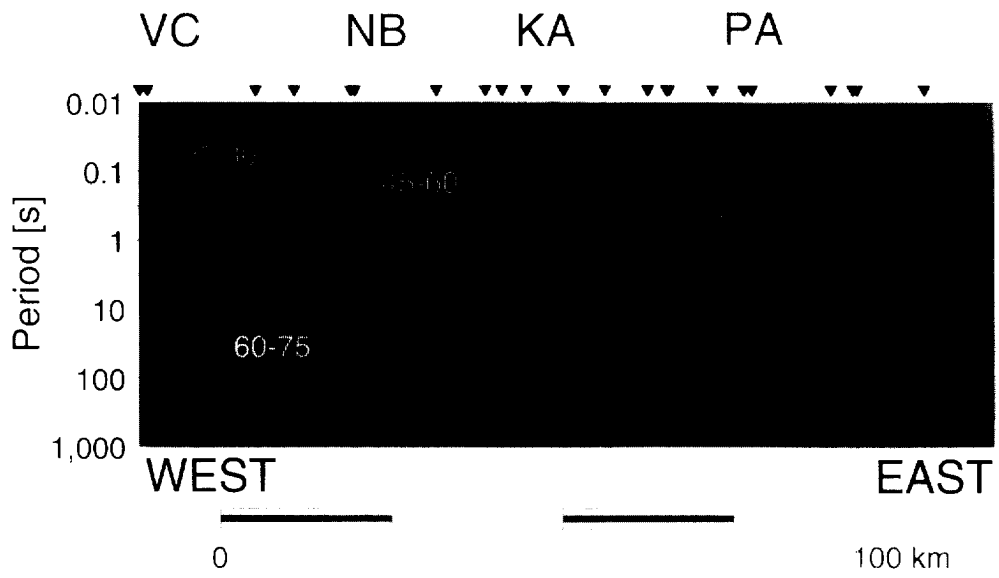

Fig. 10. Impedance phase pseudosection from sites crossing the structures in Fig. 9: *VC* = Valhalla gneiss complex; *NB* = Nelson batholith; *KA* = Kootenay Arc; *PA* = Purcell Anticlinorium; *slf* = Slocan Lake fault. High phases (>45°) signify decreasing resistivity with depth, and low phases the reverse. Note the change in phases sampling the lower crust (10–100 s) on either side of the Kootenay Arc (KA). Also, the mantle must be electrically anisotropic to explain the observations. (Adapted from Jones et al., 1993a.)

this anomaly turned from north–south to east–west to enter Hudson Bay (Gupta et al., 1985). Correlation of the location of the current with exposed geology in northern Saskatchewan and Manitoba showed that the anomalous region lay in the western part of the internides of the THO, in particular the maximum response was in the La Ronge domain, a volcano–plutonic arc domain containing metasedimentary sequences (Handa and Camfield, 1984).

Extensive MT studies have been undertaken of the NACP since the mid-1980s in Saskatchewan and the Dakotas as part of both Lithoprobe and Cocorp efforts to understand the THO. However, the first systematic study was undertaken by PanCanadian

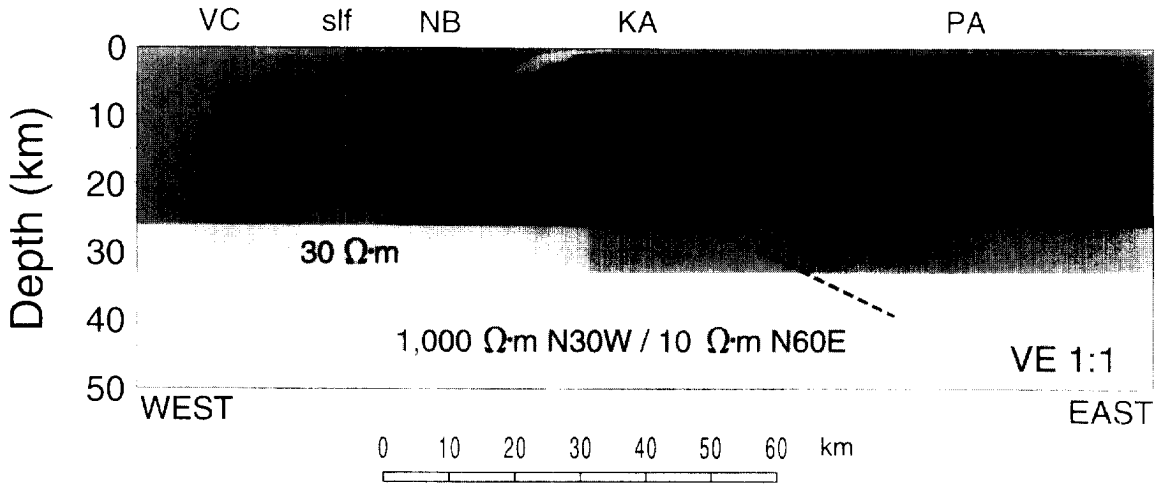

Fig. 11. Resistivity model for southeastern British Columbia: *VC* = Valhalla gneiss complex; *NB* = Nelson batholith; *KA* = Kootenay Arc; *PA* = Purcell Anticlinorium. Note the change in lower crustal resistivity on either side of the Kootenay Arc (*KA*) to explain the phase change in Fig. 10. (Adapted from Jones et al., 1993a.)

Oil Co., who were interested in the possible control of sedimentary structures in the Williston Basin by basement features (profile S in Fig. 12). This profile imaged the NACP as an arcuate, mid-crustal feature (Jones and Savage, 1986; Jones and Craven, 1990), which was later showed to drape over an Archaean microcontinent of unknown affinity (Nelson et al., 1993). The Lithoprobe seismic and MT studies in northern Saskatchewan (profiles L in Fig. 12) gave essentially the same result (Jones et al., 1993b; Lucas et al., 1993), and the model for the western part of profile L is shown in Fig. 13. An overlay of the seismic section on this model is given in Jones et al. (1993b), and the main identified structural features in the seismic data are shown as solid lines in Fig. 13. Spatial correlation confirmed the La Ronge metasediments as responsible for the NACP, and recent laboratory studies show that the anomalous conductivity is caused by pyrite grains connected along strike that have migrated to the hinges of folds (Jones et al., 1997).

The MT data image the conducting metasedimentary sequences of the La Ronge, and infer that they underlie the Rottenstone domain (RD), presumed shelf and slope-rise sequences, and the Andean-like Wathaman batholith (WB). These sediments lie structurally above a mapped late west-dipping compressional feature, the Guncoat thrust (GCT), and are interpreted to end at about the location of the surface trace of the Needles Falls shear zone (NFSZ), a late dextral fault along which tens of kilometres of displacement occurred. These sediments are juxtaposed against highly resistive rocks to the west, which probably represent the Archaean hinterland.

Tectonic models of the region invoke initial eastward(?)-directed subduction as the La Ronge arc and the Rae/Hearne craton collided, followed by a tectonic reversal and subsequent west-northwest subduction of the oceanic lithosphere between this arc–continent margin and the approaching Superior continental plate, with an intervening Archaean body of unknown derivation (Lucas et al., 1993). However, such a geometry for the initial phase would not place the metasedimentary arc sequences westward-dipping beneath the RD, but rather eastward-dipping. Accordingly, the MT model is more consistent with continuous westward-dipping subduction on this western boundary for the whole orogenesis. In addition, the model implies that the GCT is a reactivated subduction-related feature.

3.4. Example 4: imaging lithospheric mantle structures

Seismic reflection studies of the subcrustal continental lithosphere have been relatively rare, but,

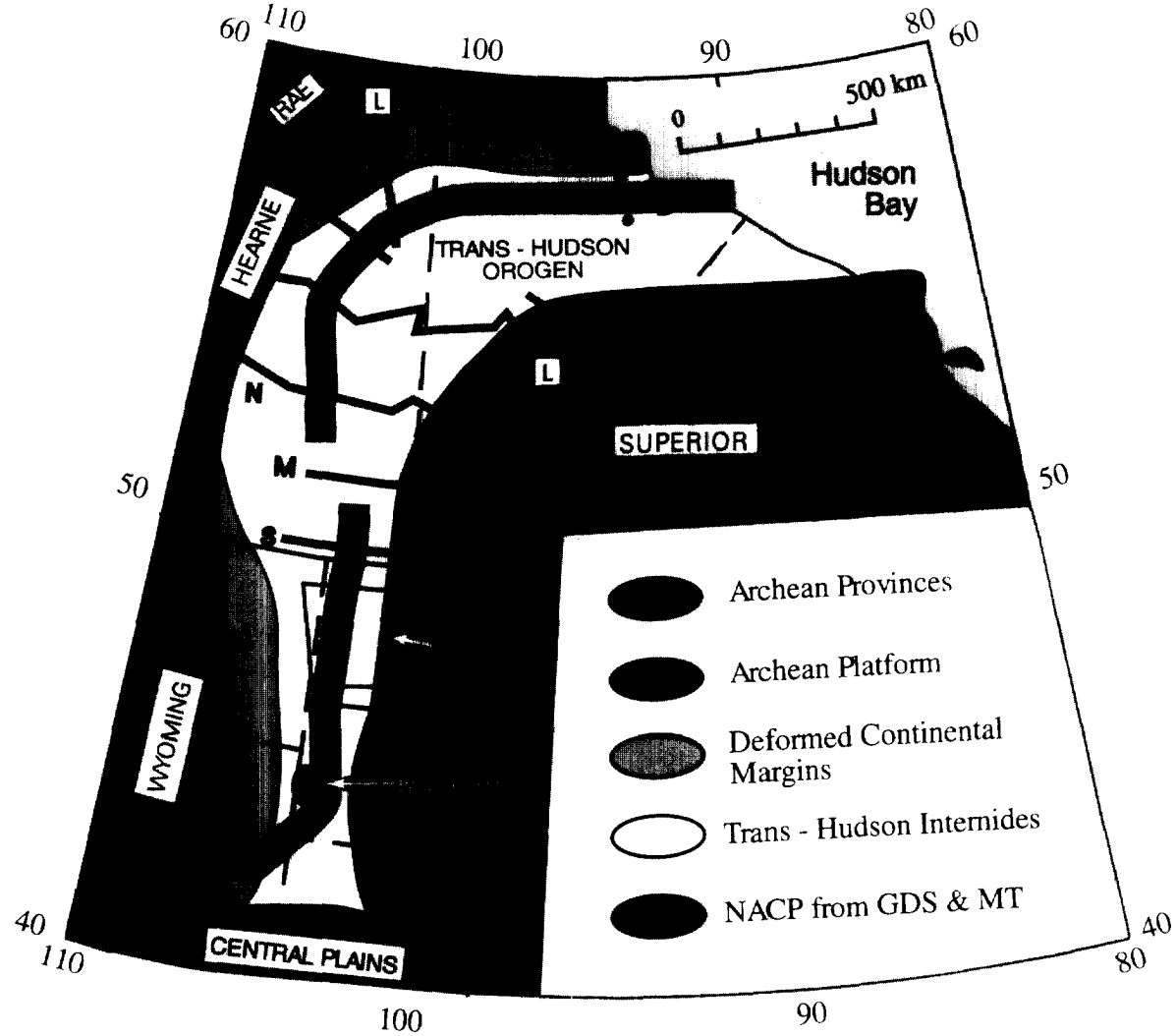

Fig. 12. Map showing trace of the North American Central Plains (*NACP*) conductivity anomaly and the Trans-Hudson orogen. MT profiles *S*, *M*, *N*, and *L*, and the North Dakota (*NOD*) survey, identified. (Adapted from Jones et al., 1993b.)

when successful, they image enigmatic features that are often considered relics of subduction zone processes, e.g., the Flannan reflector north of the British Isles (Snyder and Flack, 1990) and the Opatica reflector in the Superior Province of Canada (Calvert et al., 1995). Passive seismic methods are suited to regional mapping of the mantle in a cost-effective manner, albeit with far lower resolution. MT studies have an advantage over seismological ones since the same acquisition, analytical and numerical methods can be applied for both crustal and mantle studies (cf. reflection profiling for the crust and teleseismics for the mantle); one merely needs to use different sensors for the magnetic field to observe the lower frequencies (longer periods) and to worry about possible source-field contamination (Garcia et al., 1997).

Passive seismic studies have led to an interpretation of observed shear wave anisotropy, from shear wave phases leaving the crust–mantle boundary (predominantly SKS, more rarely PKS), in terms of aligned olivine crystallographic axis oriented in the

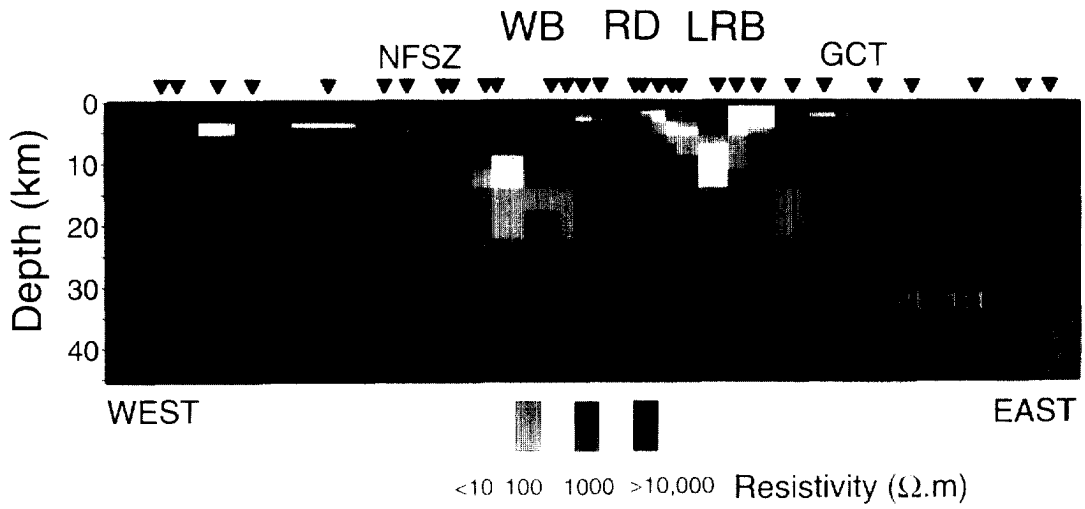

Fig. 13. Resistivity model of the western part of the Trans-Hudson orogen (vertical exaggeration 1:1). White regions have resistivity <10 S m. Black regions have resistivity > 10,000 S m. *WB* = Wathaman batholith; *RD* = Rottenstone domain; *LRB* = La Ronge belt; *NFSZ* = Needle Falls shear zone; *GCT* = Guncoat thrust. Solid lines are from the interpretation of the seismic data by Lucas et al. (1993). (Adapted from Jones et al., 1993b.)

direction of fossil stress (Silver and Chan, 1991). This interpretation has prompted a prolific rise in the number of such studies on almost all of the Earth's continents.

Until recently, there were no coincident observations of mantle electrical anisotropy to compare with seismic ones. However, impedance phase differences in orthogonal directions observed by Mareschal et al. (1995) across the Grenville Front were interpreted in terms of foliation direction (Fig. 14). A subsequent high-resolution SKS study by Senechal et al. (1996) found an obliquity between the seismic and MT-determined anisotropy directions (Fig. 14), with the fast direction estimated at N103°E (±5°) and the most conductive direction at N80°E (±6°). This was interpreted by Ji et al. (1996) as a potential indicator of fossil shearing direction, with the seismic and electrical anisotropies being controlled by lattice-preferred and shape-preferred orientations of mantle minerals (mainly olivine), respectively. The inferred dextral shearing was shown to be consistent with major faults on the surface and also with crystallographic analyses on material from a mantle xenolith.

Although the causes of both seismic and electrical anisotropy remain to be placed on a firmer foundation, clearly there is here an area that demands future effort if we are to understand the nature of the subcrustal continental lithosphere and the role that it played in the formation of the continents.

4. New directions

MT data acquisition is currently undergoing a quantum leap with the development of 24-bit systems that can acquire many tens to hundreds of channels of data (Phoenix's V5-2000, EMI's MT-24). These systems should further the use of continuous electric field acquisition such as the San Andreas fault study (Unsworth et al., 1997). For longer periods, the construction of highly sensitive, ring-core fluxgate magnetometers has led to the development of relatively cheap MT systems, such as the Geological Survey of Canada's LiMS (Long period Magnetotelluric System), which is resulting in a resurgence in projects to study the mantle. There are opportunities to design systems that record both seismic signals and electromagnetic ones for both crustal studies (reflection and continuous-dipole MT) and mantle studies (broadband seismic and long-period MT). Such systems offer significant logistical and financial advantages over independent systems.

New methods for processing the time series, such as Chave and Thomson (1998) and Larsen et al.

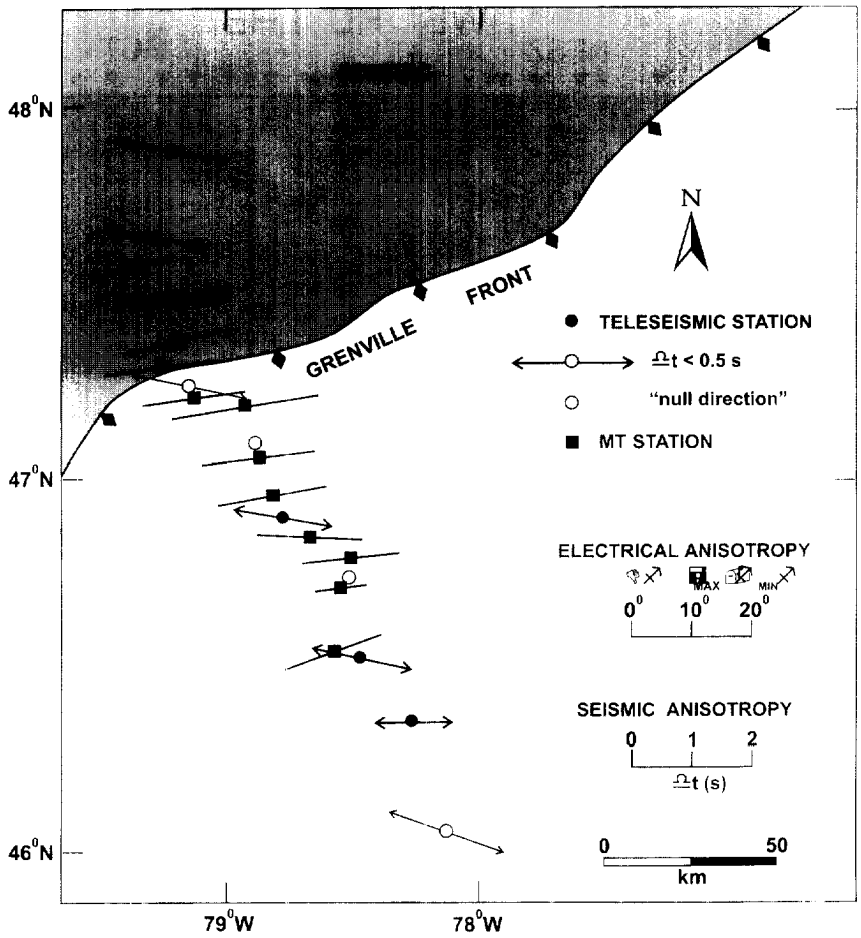

Fig. 14. Seismic and MT anisotropy information from the Superior Province of Canada. Seismic SKS time differences shown by chevroned arrows, with the average around 1.5 s and direction of +110° (±5°) MT impedance phase differences shown by plain arrows, with an average of around 20° and direction of +85° (±6°). (Adapted from Ji et al., 1996.)

(1996), result in highly precise MT response function estimates, and some of the techniques are transferrable to seismology (e.g., Jones and Holliger, 1997). Removal of near-surface 3D distortions, such as described in the MT section, are now routine. Two-dimensional inversion of the regional responses for structure has become the norm, after significant advances over the last decade with the advent of various codes (Constable et al., 1987; Smith and Booker, 1991; Agarwal et al., 1993; Oldenburg and Ellis, 1993). A comparison of various 2D forward and inverse modelling approaches applied to the same dataset can be found in Jones (1993c). Three-dimensional modelling is becoming more tractable, with fast approximate schemes such as advocated by Habashy et al. (1993), and 3D inversion will not be far behind. There have been equivalent advances in modelling and inverting seismic data. There is an untested potential for undertaking joint or cooperative modelling and inversion studies of seismic and EM data.

Finally, an area that needs addressing is laboratory studies for electrical, seismic and rheological properties of the same rock samples. In particular, the correlation of anomalous conductivity zones to regions of enhanced strain in the lithosphere addresses important rheological issues.

5. Conclusions

Science proceeds by testing hypotheses. Obviously, the more tests that can be applied to a particular hypothesis, the more convincing the hypothesis becomes. The more powerful consequence of a hypothesis failing a test is, unfortunately, considered less significant than it should be. After all, in scientific discovery, while we cannot *prove* anything, we can *falsify* a hypothesis (Popper, 1959). Unfortunately, but too few 'failures' are published.

The examples above serve to demonstrate that hypotheses built on seismological evidence can often also be tested by EM methods, and vice versa. The conclusions drawn can be profound, as in the case of the imaged partial melt zone beneath southern Tibet.

EM methods in general, and MT in particular, have now become sufficiently sophisticated that they can be used as a geological imaging tool within the arsenal at the disposal of the inquiring geoscientist. Unequivocally, there is great benefit from acquiring collocated seismic and EM data, and the number of joint studies is on the increase.

Acknowledgements

I would like to acknowledge, with gratitude, the organisers of the Asilomar workshop for their invitation to give an update on MT ten years after the last presentation (Jones, 1987). The majority of the examples I have presented come from the Canadian Lithoprobe program, and I wish to thank all my colleagues for their collaboration, in particular Fred Cook and Ron Clowes. Martyn Unsworth provided the San Andreas fault example. Reviews by Don White, David Boerner, George Jiracek, and an unknown referee, plus the comments of both editors, Walter Mooney and Simon Klemperer, are gratefully acknowledged. Geological Survey of Canada contribution No. 1996497.

References

Adam, A., 1997. Magnetotelluric phase anisotropy above extensional structure of Neogene Pannonian Basin. J. Geomagn. Geoelectr. 49, 1549–1557.

Adam, A., Szarka, L., Praeser, E., Varga, G., 1996. Mantle plumes or EM distortions in the Pannonian Basin? (Inversion of the deep magnetotelluric (MT) sounding along the Pannonian Geotraverse). Geophys. Trans. 40, 45–78.

Agarwal, A.K., Poll, H.E., Weaver, J.T., 1993. One- and two-dimensional inversion of magnetotelluric data in continental regions. Phys. Earth Planet. Inter. 81, 155–176.

Aric, K., Adam, A., Smythe, D.K., 1998. Combined seismic and magnetotelluric imaging of upper crystalline crust in the Southern Bohemian Massif. First Break (in press).

Arzate, J.A., Mareschal, M., Livelybrooks, D., 1995. Electrical image of the subducting Cocos plate from magnetotelluric observations. Geology 23, 703–706.

Arzate, J.A., Campos-Enriquez, J.O., Urrutia-Fucugauchi, J., Delgado-Rodriguez, O., 1996. Structure of the Chicxulub Impact Basin from magnetotelluric measurements. Paper presented at Fall Meeting AGU, San Francisco, December 15–19.

Bahr, K., 1984. Elimination of local 3D distortion of the magnetotelluric tensor impedance allowing for two different phases. Paper presented at Seventh Workshop on Electromagnetic Induction in the Earth and Moon, Ile-Ife, Nigeria, August 15–22.

Berdichevsky, M.N., 1960. Principles of magnetotelluric profiling theory. Appl. Geophys. (Prikl. Geofiz.) 28, 70–91.

Blackwell, D.D., Steele, J.L., Kelley, S., Korosec, M.A., 1990. Heat flow in the state of Washington and thermal conditions in the Cascade Range. J. Geophys. Res. 95, 19495–19516.

Boerner, D.E., Kurtz, R.D., Craven, J.A., Rondenay, S., Qian, W., 1995. A buried Proterozoic foredeep under the Western Canada sedimentary basin?. Geology 23, 297–300.

Booker, J.R., Aprea, C.M., Unsworth, M.J., Wu, N., 1997. Electrical conductivity structure in major continental tectonic zones. Geowissenschaften 15, 111–115.

Bostick, F.X., Smith, H.W., 1962. Investigation of large scale inhomogeneities in the Earth by the magnetotelluric method. Proc. Inst. Radio Eng. 50, 2339–2346.

Brown, L.D., Zhao, W., Nelson, K.D., Hauck, M., Alsdorf, D., Ross, A., Cogan, M., Clark, M., Liu, X., Che, J., 1997. Bright spots, structure and magmatism in southern Tibet from INDEPTH seismic reflection profiling. Science 274, 1688–1690.

Cagniard, L., 1953. Basic theory of the magneto-telluric method if geophysical prospecting [Reprinted in Vozoff (1986), pp. 4–34]. Geophysics 18, 605–635.

Calvert, A.J., Sawyer, E.W., Davis, W.J., Ludden, J.N., 1995. Archaean subduction inferred from seismic images of a mantle suture in the Superior Province. Nature 375, 670–674.

Camfield, P.A., Gough, D.I., 1977. A possible Proterozoic plate boundary in North America. Can. J. Earth Sci. 14, 1229–1238.

Caner, B., Cannon, W.H., Livingstone, C.E., 1967. Geomagnetic depth sounding and upper mantle structure in the Cordillera region of western North America. J. Geophys. Res. 72, 6335–6351.

Cassidy, J.F., Ellis, R.M., 1991. Shear wave constraints on a deep crustal reflective zone beneath Vancouver Island. J. Geophys. Res. 96, 19843–19851.

Cassidy, J.F., Ellis, R.M., 1993. S-wave velocity structure of the northern Cascadia subduction zone. J. Geophys. Res. 98, 4407–4421.

Chave, A.D., Thomson, D.J., 1998. Robust, controlled leverage processing of magnetotelluric data, Geophys. J. Int. (in press).

Chen, L., Booker, J.R., Jones, A.G., Wu, N., Unsworth, M., Wei, W., Tan, H., 1996. Electrically conductive crust in southern Tibet from INDEPTH magnetotelluric surveying. Science 274, 1694–1696.

Clarke, T.S., Burkholder, P.D., Smithson, S.B., Bentley, C.R., 1998. Optimum seismic shooting and recording parameters and a preliminary crustal model for the Byrd Subglacial Basin, Antarctica. Proc. Int. Symp. Antarct. Earth Sci., Siena (in press).

Clowes, R.M., Cook, F.A., Green, A.G., Keen, C.E., Ludden, J.N., Percival, J.A., Quinlan, G.M., West, G.F., 1993. Lithoprobe: new perspectives on crustal evolution. Can. J. Earth Sci. 29, 1813–1864.

Clowes, R.M., Zelt, C.M., Amor, J.R., Ellis, R.M., 1995. Lithospheric structure in the southern Canadian Cordillera from a network of seismic refraction lines. Can. J. Earth Sci. 32, 1485–1513.

Coleman, M.E., Parrish, R.R., 1991. Eocene dextral strike-slip and extensional faulting in the Bridge River terrane, southwest British Columbia. Tectonics 10, 1222–1238.

Constable, S.C., Parker, R.L., Constable, C.G., 1987. Occam's inversion: a practical algorithm for generating smooth models from electromagnetic sounding data. Geophysics 52, 289–300.

Constable, S., Sinha, M.C., MacGregor, L.M., Navin, D.A., Peirce, C., White, A., Heinson, G., 1997. RAMASSES finds a magma chamber beneath a slow spreading ridge. InterRidge News 6, 18–22.

Cook, F.A., 1995. Lithospheric processes and products in the southern Canadian Cordillera: a Lithoprobe perspective. Can. J. Earth Sci. 32, 1803–1824.

Cook, F.A., Jones, A.G., 1995. Seismic reflections and electrical conductivity: a case of Holmes' curious dog? Geology 23, 141–144.

Cook, F.A., Green, A.G., Simony, P.S., Price, R.A., Parrish, R.R., Milkereit, B., Gordy, P.L., Brown, R.L., Coflin, K.C., Patenaude, C., 1988. LITHOPROBE seismic reflection structure of the southeastern Canadian Cordillera: initial results. Tectonics 7, 157–180.

Cook, F.A., Varsek, J.L., Clowes, R.M., Kanasewich, E.R., Spencer, C.P., Parrish, R.R., Brown, R.L., Carr, S.D., Johnson, B.J., Price, R.A., 1992. Lithoprobe crustal reflection cross section of the southern Canadian Cordillera, 1. Foreland Thrust and Fold belt to Fraser River Fault. Tectonics 11, 12–35.

Cook, F.A., Li, Q., Vasudevan, K., 1997. Identification and interpretation of azimuthally varying crustal reflectivity with an example from the southern Canadian Cordillera. J. Geophys. Res. 102, 8447–8465.

Davey, F.J., Henyey, T., Holbrook, W.S., Okaya, D., Stern, T.A., Eberhart-Phillips, D., McEvilly, T., Urhammer, R., Anderson, H., Jiracek, G.R., Wannamaker, P.E., Caldwell, G., Christiansen, N., 1998. Preliminary results from a geophysical study across a modern, continent–continent collisional plate boundary — the Southern Alps, New Zealand. Tectonophysics (in press).

Duba, A., Heikamp, S., Meurer, W., Nover, G., Will, G., 1994. Evidence from borehole samples for the role of accessory minerals in lower-crustal conductivity. Nature 367, 59–61.

Eberhart-Phillips, D., Michael, A.J., 1993. Three-dimensional velocity structure, seismicity, and fault structure in the Parkfield region, central California. J. Geophys. Res. 98, 15737–15758.

Eberhart-Phillips, D., Stanley, W.D., Rodriguez, B.D., Lutter, W.J., 1995. Surface seismic and electric methods to detect fluids related to faulting. J. Geophys. Res. 100, 12919–12936.

Emmermann, R., Lauterjung, J., 1997. The German continental deep drilling program: overview and major results. J. Geophys. Res. 102, 18179–18201.

Everett, J.E., Hyndman, R.D., 1967. Geomagnetic variations and electrical conductivity structure in south-western Australia. Phys. Earth Planet. Inter. 1, 24–34.

Fliedner, M.M., Ruppert, S.D., Malin, P.E., Park, S.K., Jiracek, G.R., Phinney, R.A., Saleeby, J.B., Wernicke, B.P., Clayton, R.W., Keller, G.R., Miller, K.C., Jones, C.H., Luetgert, J.H., Mooney, W.D., Oliver, H.L., Klemperer, S.L., Thompson, G.A., 1996. Three-dimensional crustal structures of the southern Sierra Nevada from seismic fan profiles and gravity modelling. Geology 24, 367–370.

Forsyth, D.W., Chave, A.D., 1994. Experiment investigates magma in the mantle beneath mid-ocean ridges. EOS 75, 537–540.

Franke, W., Bortfeld, R.K., Brix, M., Drozdzewski, G., Dhrbaum, H.J., Giese, P., Janoth, W., Jödicke, H., Reichert, C., Scherp, A., Schmoll, J., Thomas, R., Thünker, M., Weber, K., Wiesner, M.G., Wong, H.K., 1990. Crustal structure of the Rhenish Massif: results of deep seismic reflection lines DEKORP 2-North and 2-North-Q. Geol. Rundsch. 79, 523–566.

Garcia, X., Chave, A.D., Jones, A.G., 1997. Robust processing of magnetotelluric data from the auroral zone. J. Geomagn. Geoelectr. 49, 1451–1468.

Gharibi, M., Korja, T., 1996. Electrical conductivity of Caledonides in Jamtland, Sweden. A poster presentation at the 13th Workshop on Electromagnetic Induction in the Earth, Onuma, Hokkaido, 12–18 July 1996 (abstr.).

Gharibi, M., Korja, T., Pedersen, L.B., 1997. Magnetotelluric study of the Caledonides in Jämtland, Sweden. Contributed paper at EGS XXII General Assembly, Vienna, 21–25 April 1997.

Gough, D.I., 1986. Seismic reflectors, conductivity, water and stress in the continental crust. Nature 323, 143–144.

Gough, D.I., 1992. Electromagnetic exploration for fluids in the Earth's crust. Earth-Sci. Rev. 32, 3–18.

Groom, R.W., Bailey, R.C., 1989. Decomposition of magnetotelluric impedance tensors in the presence of local three-dimensional galvanic distortion. J. Geophys. Res. 94, 1913–1925.

Groom, R.W., Bailey, R.C., 1991. Analytical investigations of the effects of near-surface three-dimensional galvanic scatterers on MT tensor decomposition. Geophysics 56, 496–518.

Groom, R.W., Kurtz, R.D., Jones, A.G., Boerner, D.E., 1993. A quantitative methodology for determining the dimensionality of conductive structure from magnetotelluric data. Geophys. J. Int. 115, 1095–1118.

Groupe ARMOR, 1998. Imagerie sismique et magnétotellurique

de la structure crustale du bloc Cadomien de Bretagne-Nord. C.R. Acad. Sci. Paris (in press).

Gupta, J.C., Jones, A.G., 1995. Electrical conductivity structure of the Purcell Anticlinorium in southeast British Columbia and northwest Montana. Can. J. Earth Sci. 32, 1564–1583.

Gupta, J.C., Kurtz, R.D., Camfield, P.A., Niblett, E.R., 1985. A geomagnetic induction anomaly from IMS data near Hudson Bay, and its relation to crustal electrical conductivity in central North America. Geophys. J.R. Astron. Soc. 81, 33–46.

Haak, V., Simpson, F., Bahr, K., Bigalke, J., Eisel, M., Harms, U., Hirschmann, G., Huenges, E., Jödicke, H., Kontny, A., Khek, J., Nover, G., Rauen, A., Stoll, J., Walther, J., Winter, H., Zulauf, G., 1997. KTB and the electrical conductivity of the crust. J. Geophys. Res. 102, 18289–18305.

Habashy, T.M., Groom, R.W., Spies, B.R., 1993. Beyond the Born and Rytov approximations: a nonlinear approach to electromagnetic scattering. J. Geophys. Res. 98, 1759–1775.

Hammer, P.T.C., Clowes, R.M., 1996. Seismic reflection investigations of the Mount Cayley bright spot: a mid-crustal reflector beneath the Coast Mountains, British Columbia. J. Geophys. Res. 101, 20119–20132.

Handa, S., Camfield, P.A., 1984. Crustal electrical conductivity in north-central Saskatchewan: the North American Central Plains anomaly and its relation to a Proterozoic plate margin. Can. J. Earth Sci. 21, 533–543.

Harjes, H.-P., Bram, K., Dhrbaum, H.-J., Gebrande, H., Hirschmann, G., Janik, M., Klöckner, M., Lüschen, E., Rabbel, W., Simon, M., Thomas, R., Tormann, J., Wenzel, F., 1997. Origin and nature of crustal reflections: results from integrated seismic measurements at the KTB super-deep drilling site. J. Geophys. Res. 102, 18267–18288.

Holbrook, W.S., Okaya, D.A., Henyey, T.L., Davey, F., Stern, T., 1996. Deep structure beneath the Southern Alps, New Zealand, from onshore–offshore wide-angle seismic data. Paper presented at Fall Meeting AGU, San Fransieso, December 15–19.

Hurich, C.A., Palm, H., Dyrelius, D., Kristoffersen, Y., 1989. Deformation of the Baltic continental crust during Caledonide intracontinental subduction: views from seismic reflection data. Geology 19, 423–425.

Hyndman, R.D., 1963. Electrical Conductivity Inhomogeneities in the Earth's Upper Mantle. M.Sc. thesis, Univ. British Columbia, Vancouver.

Hyndman, R.D., Vanyan, L.L., Marquis, G., Law, L.K., 1993. The origin of electrically conductive lower crust: saline water or graphite?. Phys. Earth Planet. Inter. 81, 325–344.

Ingham, M., 1996. Magnetotelluric soundings across the South Island of New Zealand: electrical structure associated with the orogen of the Southern Alps. Geophys. J. Int. 124, 134–148.

Ji, S., Rondenay, S., Mareschal, M., Senechal, G., 1996. Obliquity between seismic and electrical anisotropies as a potential indicator of movement sense for ductile mantle shear zones. Geology 24, 1033–1036.

Jiracek, G.R., 1985. Geoelectromagnetics charges on. U.S. Natl. Report to the IUGG 1991–1994. Rev. Geophys., Suppl. pp. 169–176.

Jiracek, G.R., Kinn, C.L., Scott, C.L., Nettleton, C.E., Wannamaker, P.W., 1996a. Correlation of magnetotelluric data and geothermal drilling in the Valles caldera region, New Mexico (abstr.). Expanded abstracts with bibliographies, I, 66th Annu. Int. Meet., Soc. Explor. Geophys., pp. 277–280.

Jiracek, G.R., Porter, A.D., Gonzales, V.M., Wannamaker, P.E., Stodt, J.A., Caldwell, T.G., McKnight, J.D., 1996b. Magnetotelluric investigation of continent–continent collision in the Southern Alps, New Zealand. Paper presented at Fall Meet. AGU, San Fransieso, December 15–19.

Jones, A.G., 1987. MT and reflection: an essential combination. Geophys. J. Int. 89, 7–18.

Jones, A.G., 1992. Electrical conductivity of the continental lower crust. In: Fountain, D.M., Arculus, R.J., Kay, R.W. (Eds.), Continental Lower Crust. Elsevier, Amsterdam, pp. 81–143.

Jones, A.G., 1993a. Electromagnetic images of modern and ancient subduction zones. In: Green, A.G., Kröner, A., Gotze, H.-J., Pavlenkova, N. (Eds.), Plate Tectonic Signatures in the Continental Lithosphere. Tectonophysics 219, 29–45.

Jones, A.G., 1993b. The BC87 dataset: tectonic setting, previous EM results and recorded MT data. J. Geomagn. Geoelectr. 45, 1089–1105.

Jones, A.G., 1993c. The COPROD2 dataset: tectonic setting, recorded MT data and comparison of models. J. Geomagn. Geoelectr. 45, 933–955.

Jones, A.G., Craven, J.A., 1990. The North American Central Plains conductivity anomaly and its correlation with gravity, magnetics, seismic, and heat flow data in the Province of Saskatchewan. Phys. Earth Planet. Inter. 60, 169–194.

Jones, A.G., Dumas, I., 1993. Electromagnetic images of a volcanic zone. Phys. Earth Planet. Inter. 81, 289–314.

Jones, A.G., Gough, D.I., 1995. Electromagnetic studies in southern and central Canadian Cordillera. Can. J. Earth Sci. 32, 1541–1563.

Jones, A.G., Holliger, K., 1997. Spectral analysis of the KTB sonic and density logs using robust nonparametric methods. J. Geophys. Res. 102, 18391–18403.

Jones, A.G., Savage, P.J., 1986. North American Central Plains conductivity anomaly goes east. Geophys. Res. Lett. 13, 685–688.

Jones, A.G., Kurtz, R.D., Oldenburg, D.W., Boerner, D.E., Ellis, R., 1988. Magnetotelluric observations along the LITHOPROBE southeastern Canadian Cordilleran transect. Geophys. Res. Lett. 15, 677–680.

Jones, A.G., Kurtz, R.D., Boerner, D.E., Craven, J.A., McNeice, G., Gough, D.I., DeLaurier, J.M., Ellis, R.G., 1992. Electromagnetic constraints on strike-slip fault geometry — the Fraser River fault system. Geology 20, 561–564.

Jones, A.G., Groom, R.W., Kurtz, R.D., 1993a. Decomposition and modelling of the BC87 dataset. J. Geomagn. Geoelectr. 45, 1127–1150.

Jones, A.G., Craven, J.A., McNeice, G.A., Ferguson, I.J., Boyce, T., Farquharson, C., Ellis, R.G., 1993b. The North American Central Plains conductivity anomaly within the Trans-Hudson orogen in northern Saskatchewan. Geology 21, 1027–1030.

Jones, A.G., Katsube, J., Schwann, P., 1997. The longest conductivity anomaly in the world explained: sulphides in fold

hinges causing very high electrical anisotropy. J. Geomagn. Geoelectr. (in press).

Kirkwood, S.C., Hutton, V.R.S., Sik, J., 1981. A geomagnetic study of the Great Glen fault. Geophys. J.R. Astron. Soc. 66, 481–490.

Klein, D.P., 1991. Crustal resistivity structure from magnetotelluric soundings in the Colorado Plateau–Basin and Range provinces, central and western Arizona. J. Geophys. Res. 96, 12313–13331.

Korja, A., Korja, T., Luosto, U., Heikkinen, P., 1993. Seismic and geoelectric evidence for collisional and extensional events in the Fennoscandian Shield: implications for Precambrian crustal evolution. Tectonophysics 219, 129–152.

Korja, T., Tuisku, P., Pernu, T., Karhu, J., 1996. Lapland Granulite Belt — implications for properties and evolution of deep continental crust. Terra Nova 8, 48–58.

Kurtz, R.D., DeLaurier, J.M., Gupta, J.C., 1986. A magnetotelluric sounding across Vancouver Island sees the subducting Juan de Fuca plate. Nature 321, 596–599.

Kurtz, R.D., DeLaurier, J.M., Gupta, J.C., 1990. The electrical conductivity distribution beneath Vancouver Island: a region of active plate subduction. J. Geophys. Res. 95, 10929–10946.

Lahiri, B.N., Price, A.T., 1939. Electromagnetic induction in non-uniform conductors, and the determination of the conductivity of the Earth from terrestrial magnetic variations. Philos. Trans. R. Soc. London, Ser. A 237, 509–540.

Lajoie, J.J., Caner, B., 1970. Geomagnetic induction anomaly near Kootenay Lake — a strike-slip feature in the lower crust?. Can. J. Earth Sci. 7, 1568–1579.

Larsen, J.C., Mackie, R.L., Manzella, A., Fiordelisi, A., Rieven, S., 1996. Robust smooth magnetotelluric transfer functions. Geophys. J. Int. 124, 801–819.

Leclair, A.D., Percival, J.A., Green, A.G., Wu, J.J., West, G.F., Wang, W., 1994. Seismic reflection profiles across the central Kapuskasing uplift. Can. J. Earth Sci. 31, 1016–1026.

Lucas, S.B., Green, A.G., Hajnal, Z., White, D., Lewry, J., Ashton, K., Weber, W., Clowes, R., 1993. Deep seismic profile across a Proterozoic collision zone: surprises at depth. Nature 363, 339–342.

Lutter, W.J., Roberts, P.M., Thurber, C.H., Steck, L., Fehler, M.C., Stafford, D.G., Baldridge, W.S., Zeichert, T.A., 1995. Teleseismic P-wave image of crust and mantle structure beneath the Valles caldera, New Mexico: initial results from the 1993 JTEX passive array. Geophys. Res. Lett. 22, 505–508.

Mackie, R.L., Livelybrooks, D.W., Madden, T.R., Larsen, J.C., 1996. A magnetotelluric investigation of the San Andreas fault at Carrizo Plain, California. Geophys. Res. Lett. (in press).

Makovsky, Y., Klemperer, S.L., Ratschbacher, L., Brown, L.D., Li, M., Zhao, W., Meng, F., 1997. INDEPTH wide-angle reflection observation of P-wave to S-wave conversion from crustal bright spots in Tibet. Science 274, 1690–1691.

Mareschal, M., Kurtz, R.D., Bailey, R.C., 1994. A review of electromagnetic investigations in the Kapuskasing uplift and surrounding regions: electrical properties of key rocks. Can. J. Earth Sci. 31, 1042–1051.

Mareschal, M., Kellett, R.L., Kurtz, R.D., Ludden, J.N., Bailey, R.C., 1995. Archean cratonic roots, mantle shear zones and deep electrical anisotropy. Nature 373, 134–137.

Marquis, G., Jones, A.G., Hyndman, R.D., 1995. Coincident conductive and reflective lower crust across a thermal boundary in southern British Columbia, Canada. Geophys. J. Int. 120, 111–131.

McCarthy, J., Larkin, S.P., Fuis, R.W., Simpsom, R.W., Howard, K.A., 1991. Anatomy of a metamorphic core complex: seismic refraction/wide-angle reflection profiling in southeastern California and western Arizona. J. Geophys. Res. 96, 12259–12291.

McLean, N.A., 1995. Crustal Seismic Velocity Structure of the Intermontane and Coast belts, Southwestern Canadian Cordillera. M.Sc. thesis, Univ. Victoria, Victoria, B.C., 110 pp.

McNeice, G.W., Jones, A.G., 1996. Multisite, multifrequency tensor decomposition of magnetotelluric data. Oral presentation, 66th Soc. Explor. Geophys. Meet., Denver, Colo., 10–15 November, Publ. in Abstract Proceedings, pp. 281–284.

Meltzer, A.S., Zeitler, P.K., Schoemann, M.L., Beaudoin, B.C., Seeber, L., Armbruster, J.G., 1996. The Nanga Parbat Seismic Experiment. Paper presented at Fall Meet. AGU, San Francisco, December 15–19.

Migaux, L., Astier, J.L., Reval, P.H., 1960. Un essai de détermination expérimentale de la résistivité électrique des couches profondes de l'écorce terrestre. Ann. Geophys. 16, 555–560.

Nelson, K.D., Baird, D.J., Walters, J.J., Hauck, M., Brown, L.D., Oliver, J.E., Ahern, J.L., Hajnal, Z., Jones, A.G., Sloss, L.L., 1993. Trans-Hudson orogen and Williston basin in Montana and North Dakota: New COCORP deep profiling results. Geology 21, 447–450.

Nelson, K.D., Wenjin Zhao, Brown, L.D., Kuo, J., Jinkai Che, Xianwen Liu, Klemperer, S.L., Makovsky, Y., Meissner, R., Mechie, J., Kind, R., Wenzel, F., Ni, J., Nabelek, J., Leshou Chen, Handong Tan, Wenbo Wei, Jones, A.G., Booker, J., Unsworth, M., Kidd, W.S.F., Hauck, M., Alsdorf, D., Ross, A., Cogan, M., Changde Wu, Sandvol, E., Edwards, M., 1996. Partially molten middle crust beneath southern Tibet: synthesis of Project INDEPTH results. Science 274, 1684–1688.

Nesbitt, B.E., Muehlenbachs, K., 1991. Stable isotopic constraints on the nature of the syntectonic fluid regime of the Canadian Cordillera. Geophys. Res. Lett. 18, 963–966.

Neves, A.S., 1957. The Magnetotelluric Method in Two-dimensional Structures. Unpubl. Ph.D. thesis, Mass. Inst. Technol., Cambridge, Mass.

Oldenburg, D.W., Ellis, R.G., 1993. Efficient inversion of magnetotelluric data in two dimensions. Phys. Earth Planet. Inter. 81, 177–200.

Olhoeft, G.R., 1981. Electrical properties of granite with implications for the lower crust. J. Geophys. Res. 86, 931–936.

Park, S.K., Mackie, R.L., 1996. Interpretation of three-dimensional MT data — case study along the Indus River, northern Pakistan. Paper presented at Fall Meet. AGU, San Francisco, December 15–19.

Park, S.K., Biasi, G.P., Mackie, R.L., Madden, T.D., 1991. Magnetotelluric evidence for crustal suture zones bounding the

southern Great Valley, California. J. Geophys. Res. 96, 353–376.

Percival, J.A., West, G.F., 1994. The Kapuskasing uplift: a geological and geophysical synthesis. Can. J. Earth Sci. 31, 1256–1286.

Perz, M.J., 1993. Characteristics of the Fraser Fault, Southwestern British Columbia, and Surrounding Geology through Reprocessing of Seismic Reflection Data. M.Sc. thesis, Univ. British Columbia, Vancouver, B.C., 191 pp.

Phinney, R.A., Silver, P., Lerner-Lam, A., Park, J., Carlson, R., 1993. A National Report for Research in Continental Dynamics — CD/2020. Publ. by. IRIS Corp., Virginia, 72 pp.

Popper, K.R., Sir, 1959. The Logic of Scientific Discovery. Univ. Toronto Press., 479 pp.

Posgay, K., Takacs, E., Szalay, I., Bodoky, T., Hegedus, E., Kantor, I.J., Timar, Z., Varga, G., Berczi, I., Szalay, A., Nagy, Z., Papa, A., Hajnal, Z., Reilkoff, B., Mueller, S., Ansorge, J., De Iaco, R., Asudeh, I., 1996. International deep reflection survey along the Hungarian Geotraverse. Geophys. Trans. 40, 1–44.

Pous, J., Queral, P., Ledo, J., Garcia-Duenas, V., Sallares, V., Danobeitia, J.J., Carbonell, R., 1996. Coincident reflectivity and high electrical conductivity beneath the Betics mountain chain. Paper presented at 7th Int. Symp. Deep Seismic Profiling Cont., Asilomar, Calif., Sept. 15–22.

Price, R.A., Carmichael, D.M., 1986. Geometric test for late Cretaceous–Paleogene intracontinental transform faulting in the Canadian Cordillera. Geology 14, 468–471.

Ross, G.M., Milkereit, B., Eaton, D., White, D., Kanasewich, E.R., Burianyk, J.A., 1995. Paleoproterozoic collisional orogen beneath western Canada sedimentary basin imaged by Lithoprobe crustal seismic-reflection data. Geology 23, 195–199.

Senechal, G., Rondenay, S., Mareschal, M., Guilbert, J., Poupinet, G., 1996. Seismic and electrical anisotropies in the lithosphere across the Grenville Front, Canada. Geophys. Res. Lett. 23, 2255–2258.

Shankland, T.J., Ander, M.E., 1983. Electrical conductivity, temperatures, and fluids in the lower crust. J. Geophys. Res. 88, 9475–9484.

Simpson, F., and the KRISP MT Working Group, 1996. Electromagnetic properties of the southern Kenyan Rift and the Chyulu volcanic range. Paper presented at 13th Workshop on Electromagnetic Induction in the Earth, Onuma, July 12–18.

Sinha, M.C., Navin, D.A., MacGregor, L.M., Constable, S., Peirce, C., White, A., Heinson, G., Inglis, M.A., 1997. Evidence for accumulated melt beneath the slow-spreading mid-Atlantic ridge. Philos. Trans. R. Soc. London 355, 233–253.

Silver, P.G., Chan, W.W., 1991. Shear-wave splitting and subcontinental mantle deformation. J. Geophys.Res. 96, 16429–16454.

Smith, J.T., Booker, J.R., 1991. Rapid inversion of two and three-dimensional magnetotelluric data. J. Geophys. Res. 96, 3905–3922.

Snyder, D.B., Flack, C.A., 1990. A Caledonian age for reflectors within the mantle lithosphere north and west of Scotland. Tectonics 9, 903–922.

Stern, T.A., Wannamaker, P.E., Eberhart-Phillips, D., Okaya, D., Davey, F.J., the South Island working group, 1998. Crustal structure experiments across the Southern Alps of New Zealand. EOS, Trans. AGU (in press).

Stoerzel, A., Smithson, S.B., 1996. Seismic structure of the Ruby mountains core complex, eastern Nevada, from multicomponent seismic wide-angle data. Paper presented at 7th Int. Symp. Deep Seismic Profiling Cont., Asilomar, Calif., Sept. 15–22.

Swift, C.M., 1967. A Magnetotelluric Investigation of an Electrical Conductivity Anomaly in the South-Western United States. Unpubl. Ph.D. thesis, Dept. Geology Geophys., Mass. Inst. Technol., Cambridge, Mass.

Tikhonov, A.N., 1950. On the determination of the electric characteristics of deep layers of the Earth's crust [Reprinted in Vozoff (1986), pp. 2–3]. Dokl. Akad. Nauk SSSR 73, 295–297.

Trehu, A.M., Asudeh, I., Brocher, T.M., Luetgert, J.H., Mooney, W.D., Nabelek, J.L., Nakamura, Y., 1994. Crustal architecture of the Cascadia Forearc. Science 265, 237–243.

Tyburczy, J.A., Waff, H.S., 1983. Electrical conductivity of molten basalt and andesite to 25 kilobars pressure: geophysical significance and implications for charge transport and melt structure. J. Geophys. Res. 88, 2413–2430.

Unsworth, M.J., Malin, P.E., Egbert, G.D., Booker, J.R., 1997. Internal structure of the San Andreas Fault at Parkfield, California. Geology 25, 359–362.

Varsek, J.L., Cook, F.A., Clowes, R.M., Journeay, J.M., Monger, J.W.H., Parrish, R.R., Kanasewich, E.R., Spencer, C.P., 1993. LITHOPROBE crustal reflection structure of the southern Canadian Cordillera II: Coast Mountains transect. Tectonics 12, 334–360.

Volbers, R., Joedicke, H., Untiedt, J., 1990. Magnetotelluric study of the earth's crust along the deep seismic reflection profile DEKORP 2-N. Geol. Rundsch. 79, 581–601.

Vozoff, K. (Ed.), 1986. Magnetotelluric Methods. Soc. Expl. Geophys. Reprint Ser. No. 5, Soc. Explor. Geophys., Tulsa, Okla.

Vozoff, K., 1991. The magnetotelluric method. In: Electromagnetic Methods in Applied Geophysics — Applications. Soc. Explor. Geophys., Tulsa, Okla., pp. 641–712.

Wannamaker, P.E., Booker, J.R., Filloux, J.H., Jones, A.G., Jiracek, G.R., Chave, A.D., Waff, H.S., Young, C.T., Stodt, J.A., Martinez, M., Law, L.K., Yukitake, T., Segawa, J.S., White, A., Green, A.W., 1989a. Magnetotelluric observations across the Juan de Fuca subduction system in the EMSLAB project. J. Geophys. Res. 94, 14121–14125.

Wannamaker, P.E., Booker, J.R., Jones, A.G., Chave, A.D., Filloux, J.H., Waff, H.S., Law, L.K., 1989b. Resistivity cross-section through the Juan de Fuca subduction system and its tectonic implications. J. Geophys. Res. 94, 14127–14144.

Wannamaker, P.E., Stodt, J.A., Olsen, S.L., 1996. Dormant state of rifting below the Byrd Subglacial Basin, West Antarctica, implied by magnetotelluric profiling. Geophys. Res. Lett. 23, 2983–2986.

Wernicke, B.P., Clayton, R.W., Ducea, M.N., Jones, C.H., Park, S.K., Ruppert, S.D., Saleeby, J.B., Snow, J.K., Squires, L.J.,

Fliedner, M.M., Jiracek, G.R., Keller-, G.R., Klemperer, S.L., Luetgert, J.H., Malin, P.E., Miller, K.C., Mooney, W.D., Oliver, H.W., Phinney, R.A., 1996. Origin of high mountains in the continents; the southern Sierra Nevada. Science 271, 190–193.

Yardley, B.W.D., Valley, J.W., 1997. The petrologic case for a dry lower crust. J. Geophys. Res. 102, 12172–12185.

Zelt, C.A., White, D.J., 1995. Crustal structure and tectonics of the southeastern Canadian Cordillera. J. Geophys. Res. 100, 24255–24273.